

Alma Mater Studiorum Università di Bologna
Archivio istituzionale della ricerca

Neutral Re(I) Complex Platform for Live Intracellular Imaging

This is the final peer-reviewed author's accepted manuscript (postprint) of the following publication:

Published Version:

Gillam, T.A., Caporale, C., Brooks, R.D., Bader, C.A., Sorvina, A., Werrett, M.V., et al. (2021). Neutral Re(I) Complex Platform for Live Intracellular Imaging. INORGANIC CHEMISTRY, 60(14), 10173-10185 [10.1021/acs.inorgchem.1c00418].

Availability:

This version is available at: <https://hdl.handle.net/11585/831928> since: 2021-09-10

Published:

DOI: <http://doi.org/10.1021/acs.inorgchem.1c00418>

Terms of use:

Some rights reserved. The terms and conditions for the reuse of this version of the manuscript are specified in the publishing policy. For all terms of use and more information see the publisher's website.

This item was downloaded from IRIS Università di Bologna (<https://cris.unibo.it/>).
When citing, please refer to the published version.

(Article begins on next page)

This is the final peer-reviewed accepted manuscript of:

Neutral Re(I) complex platform for live intracellular imaging

by: Todd A. Gillam, Chiara Caporale, Robert D. Brooks, Christie A. Bader, Alexandra Sorvina, Melissa V. Werrett, Phillip J. Wright, Janna L. Morrison, Massimiliano Massi, Doug A. Brooks, Stefano Zacchini, Shane M. Hickey, Stefano Stagni, and Sally E. Plush, *Inorganic Chemistry*, **2021**, 60, 10173-10185.

The final published version is available online at:
<https://doi.org/10.1021/acs.inorgchem.1c004183>.

Rights / License: CCBYNCND

The terms and conditions for the reuse of this version of the manuscript are specified in the publishing policy. For all terms of use and more information see the publisher's website.

This item was downloaded from IRIS Università di Bologna (<https://cris.unibo.it/>)

When citing, please refer to the published version.

Neutral Re(I) complex platform for live intracellular imaging

*Todd A. Gillam,[a,d] Chiara Caporale,[b] Robert D. Brooks,[a] Christie A. Bader,[a]
Alexandra Sorvina,[a]Melissa V. Werrett, [c] Phillip J. Wright,[b] Janna L. Morrison,[a]
Massimiliano Massi,[b] Doug A. Brooks,[a] Stefano Zacchini,[e] Shane M. Hickey,[a]
Stefano Stagni,[e]* and Sally E. Plush[a,d]**

a UniSA Clinical and Health Sciences, University of South Australia, North Tce, Adelaide,
SA 5000, Australia.

b Department of Chemistry, Curtin University, Kent St., Bentley, WA 6102, Australia.

c School of Chemistry, Monash University, Clayton, Melbourne, Victoria 3800, Australia.

d UniSA STEM, Future Industries Institute, University of South Australia, Mawson Lakes,
SA 5095, Australia.

e Department of Industrial Chemistry “Toso Montanari”, University of Bologna, Viale
Risorgimento, 4, Bologna 40136, Italy.

*equal corresponding authors

Email: sally.plush@unisa.edu.au, stefano.stagni@unibo.it

Abstract: Luminescent metal complexes are a valuable platform for the generation of cell imaging agents. However, many metal complexes are cationic, a factor which can dominate the intracellular accumulation to specific organelles. Neutral Re(I) complexes offer a more attractive platform for the development of bioconjugated imaging agents where charge cannot influence their intracellular distribution. Herein, we report the synthesis of a neutral complex (**ReAlkyne**), which was used as a platform for the generation of four carbohydrate-conjugated imaging agents *via* copper(I)-catalyzed azide-alkyne cycloaddition. A comprehensive evaluation of the physical and optical properties of each complex is provided, together with a determination of their utility as live cell imaging agents in H9c2 cardiomyoblasts. Unlike their cationic counter parts, many of which localize within mitochondria, these neutral complexes have localized within the endosomal/lysosomal network, a result consistent with examples of dinuclear neutral carbohydrate appended Re(I) complexes which have been reported. This further demonstrates the utility of this neutral Re(I) complex imaging platforms as viable imaging platforms for the development of bioconjugated cell imaging agents

Introduction

Imaging agents can be used to trace the cellular uptake, transport and sequestration of biomolecules, revealing valuable insights into cell biology.¹⁻² Emissive transition metal complexes provide an ideal platform for the development of luminescent live cell imaging agents as they exhibit high quantum yields, possess long-lived visible emission (> 100 ns) and are resistant to photobleaching.³⁻⁴ These live cell imaging agents are mainly based on cationic transition metal complexes of Ir(III), Re(I) or Ru(II),⁵⁻¹¹ which have excellent photophysical properties, but can exhibit cytotoxicity (an effect that has been ascribed to the cationic charge).^{7, 12-13} Moreover, charged complexes often localize within mitochondria,¹³⁻¹⁶ and are therefore not suitable for the wider application of a ligand-targeted imaging platform. Neutral Re(I) complexes have proven to be highly biocompatible, imparting minimal cytotoxicity and enabling live cell imaging applications, without an inherent tendency to localize within mitochondria.¹⁷⁻²² The low toxicity and photophysical properties of neutral Re(I) complexes make them attractive for the development of novel and targeted imaging agent technologies that do not disturb delicate cell biological processes.

Carbohydrate-conjugated metal complexes comprise some of the earliest examples of bioconjugation.¹³ With the exception of some multivalent neutral glucose conjugated Re complexes developed by Palmioli *et. al*,²¹⁻²² the vast majority of carbohydrate-conjugated complexes are cationic complexes of Ir(III), Re(I) or Ru(II), several of which have been used as imaging agents in cancer cells.^{10, 13-15} More specifically, conjugation of β -glucose to a cationic Re(I) scaffold results in greater cellular uptake by HeLa and MCF-7 cells, compared to HEK293T and NIH/3T3 cells, which has been ascribed to the involvement of an active carbohydrate mediated uptake mechanism.^{10, 13} However, these imaging agents accumulated in mitochondria and caused

cytotoxicity as a result of the inherent cationic nature and lipophilicity of the complex.¹³ Fructose-appended cationic cyclometalated Ir(III) complexes have also displayed elevated uptake by malignant cells (i.e. HeLa cells), mitochondrial accumulation and a poor cytotoxicity profile;¹⁴ as have cationic Ir(III) conjugates of glucose, galactose, lactose and maltose.¹⁵ In these instances, the cationic nature of the complex is presumed to drive the mitochondrial distribution, as opposed to any effects imparted by the carbohydrate motifs. Contrastingly, reported carbohydrate appended neutral Re(I) complexes have been reported to localize within the endosomal network without mitochondrial accumulation (in instances where intracellular localization was assessed).²¹ With our ongoing interest in developing neutral Re(I) complexes, we set out to synthesize a series of proof-of-principle biocompatible live cell imaging agents by functionalizing neutral Re(I) complexes with different carbohydrate moieties.

From a common Re(I)-based building block equipped with an alkyne handle (**ReAlkyne**), we report the modular synthesis of four novel imaging agents, each conjugated with a different carbohydrate whose selection is justified by their previous use as effective bioconjugates of cationic and neutral complexes in the literature (**Figure 1**).^{13, 15, 21, 23-25} A comprehensive evaluation of the photophysical properties of each complex was conducted, which is relevant to their potential performance as cellular imaging agents. Cellular uptake studies of the sugar conjugated Re(I) complexes and biodistribution were assessed in H9c2 cardiomyoblasts, a cell line that is proliferative and highly dependent on carbohydrate metabolism, displaying distinct metabolic features amenable to the evaluation of carbohydrate utilization.²⁶

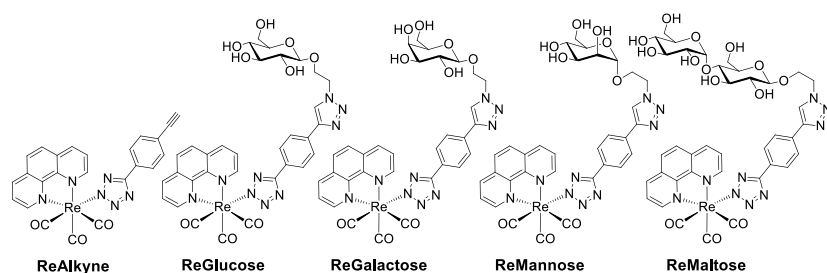


Figure 1. Structures of the ReAlkyne platform and four carbohydrate-conjugated Re(I) complexes.

Experimental Section

General Measurements and Analysis Instrumentation. All reagents and solvents were purchased from Sigma-Aldrich, Alfa Aesar or Merck and were used as received. Anhydrous DMF was purchased from Sigma-Aldrich. Anhydrous CH_2Cl_2 and MeOH were prepared by drying over freshly activated 3 Å molecular sieves. All reactions performed above ambient temperatures were conducted using a heating mantle. All ^1H and ^{13}C NMR spectra were collected at 298 K on either a Bruker AVANCE III 500 MHz, a Bruker Avance 400 MHz, or a Varian Mercury Plus 400 MHz FT-NMR spectrometer. Samples were dissolved in CDCl_3 or CD_3OD , with the residual solvent peak used as the internal reference: DMSO- d_6 2.50 (^1H) and 39.72 (^{13}C); CDCl_3 ; 7.26 (^1H) and 77.0 (^{13}C); CD_3OD ; 3.31 (^1H) and 49.0 (^{13}C); and acetone- d_6 ; 2.05 (^1H) and 29.84 (^{13}C).²⁷ High resolution mass spectra (HRMS) were recorded on an AB SCIEX TripleTOF 5600 mass spectrometer, and ionization of all samples was carried out using electrospray ionization (ESI). Analyte solutions were prepared in HPLC grade MeOH or CH_3CN (concentration ≈ 1 mg/mL). Melting points were determined using a Stuart SMP10 melting point apparatus and are uncorrected. Infrared spectra (IR) were recorded on solid-state samples using an attenuated total reflectance Perkin Elmer Spectrum Two and Spectrum100 FT-IR. The purity of compounds used for biological evaluation was determined by analytic RP-HPLC, which was carried out on a

Shimadzu Prominence UltraFast Liquid Chromatograph (UFLC) system equipped with a CBM-20A communications bus module, a DGU-20A5R degassing unit, a LC-20AD liquid chromatograph pump, a SIL-20AHT auto-sampler, a SPD-M20A photo diode array detector, a CTO-20A column oven and an Alltech Platinum EPS C18 100A 5 μ 250 \times 4.6 mm column. Method A (gradient 5% to 95% MeOH in H₂O containing 0.1% formic acid (FA) over 7 min at a flow rate of 1 mL/min, followed by 95% MeOH in H₂O containing 0.1% FA over 13 min) and method B (gradient 5% to 95% CH₃CN in H₂O containing 0.1% FA over 7 min at a flow rate of 1 mL/min, followed by 95% CH₃CN in H₂O containing 0.1% FA over 13 min) were used for analytic RP-HPLC. Thin layer chromatography (TLC) was performed on Merck silica gel 60 F₂₅₄ pre-coated aluminum plates (0.2 mm) and visualized using UV light (λ = 254 nm) and/or a KMnO₄ oxidizing stain (KMnO₄, H₂O and K₂CO₃). Column chromatography was performed on silica gel GRACE Davison DAVISIL[®] silica gel 60 Å (230-400 mesh) and Alfa Aesar, Aluminium oxide activated neutral Brockman grade I, 58 Å. Compounds **1** and **2** were prepared following literature procedures and are described in the ESI.²⁸⁻³⁰

Caution: NaN₃ has the potential to form explosive mixtures, it should be handled with care and all halogenated solvents should be avoided.

Synthesis of the ReAlkyne platform:

fac-[Re(phen)(CO)₃(TIod)] (**3**)

To a stirring solution of **2** (100 mg, 0.13 mmol) EtOH/H₂O (3:1, 20 mL) was added dropwise a solution of **1** (54 mg, 0.20 mmol) and Et₃N (28 μ L, 0.20 mmol) in EtOH/H₂O (3:1, 5 mL) at ambient temperature under an atmosphere of argon. The reaction mixture was then heated at reflux for 24 h before cooling to ambient temperature. The reaction mixture was filtered using vacuum

filtration to isolate the title complex as a yellow solid (70 mg, 71%). ν_{\max} (IR)/ cm^{-1} , CH_2Cl_2 , rt: 2029 s (CO, A'(1)), 1924 s br (CO, A'(2)/A''). ^1H NMR (δ , ppm, CDCl_3 , 400 MHz): 9.53 (2H, d, $J = 6.4$ Hz, phen), 8.56 (2H, d, $J = 8.4$ Hz, phen), 8.00 (2H, s, phen), 7.91–7.87 (2H, m, phen), 7.58 (2H, d, $J = 8.0$ Hz, *Tphl*), 7.53 (2H, d, $J = 8.0$ Hz, *Tphl*); ^{13}C NMR (δ , ppm, CDCl_3 , 100 MHz): 196.5, 193.6, 162.7, 153.8, 147.6, 138.4, 137.3, 130.5, 129.4, 128.1, 127.5, 125.9. HRMS (ESI, m/z) for $\text{C}_{22}\text{H}_{13}\text{IN}_6\text{O}_3\text{Re}$ [$\text{M} + \text{H}$] $^+$ calc. 722.9704; found 722.9711.

ReAlkyne

To a stirring mixture of **3** (200 mg, 0.277 mmol), *cis*-[Pd(PPh₃)₂Cl₂] (40 mg, 0.055 mmol) and CuI (10 mg, 0.055 mmol) in freshly distilled THF (8 mL) under an atmosphere of argon at ambient temperature, was sequentially added Et₃N (8 mL, 57.36 mmol) and ethynyltrimethylsilane **4** (115 μL , 0.831 mmol) and heated at reflux for 24 h. The reaction mixture was cooled to ambient temperature, filtered over Celite and the filtrate was concentrated under reduced pressure. The crude reaction mixture was suspended in CH_2Cl_2 and passed through a plug of Al_2O_3 on sintered glass to remove residual Pd and Cu species. The filtrate was concentrated under reduced pressure and the crude material added to a suspension of K₂CO₃ (30 mg, 0.217 mmol) in MeOH (15 mL) and stirred under an atmosphere of argon at ambient temperature for 24 h. The suspension was then concentrated under reduced pressure and partitioned with CH_2Cl_2 (15 mL) and H₂O (15 mL) and separated, the organic extract was collected and washed a further two times with H₂O. The organic extract was dried with Na₂SO₄ and concentrated under reduced pressure. The crude material was obtained as a yellow residue, and following purification by column chromatography on Al_2O_3 with CH_2Cl_2 /acetone (9:1), **ReAlkyne** was obtained as a yellow crystalline solid (105 mg, 61%). ν_{\max} (IR)/ cm^{-1} , CH_2Cl_2 : 2029 s (CO, A'(1)), 1923 s br (CO, A'(2)/A''). ^1H NMR (400 MHz, Acetone-*d*₆): δ 3.50 (1H, s, CN₄-C₆H₄-C \equiv CH), 7.36 (2H, d, $J = 8.8$ Hz, CN₄-C₆H₄-

C≡CH), 7.64 (2H, d, $J = 8.0$ Hz, CN₄-C₆H₄-C≡CH), 8.16–8.20 (2H, m, phen), 8.31 (2H, s, phen), 8.97 (2H, d, $J = 8.4$ Hz, phen), 9.66 (2H, d, $J = 5.4$ Hz, phen), ¹³C NMR (100 MHz, Acetone-*d*₆): δ 197.3, 195.6, 163.0, 155.1, 148.2, 140.4, 132.8, 131.7, 131.6, 128.7, 127.4, 126.6, 122.7 84.1, 79.7. HRMS (ESI, m/z) for C₂₄H₁₄N₆O₃Re [M + H]⁺ calc. 621.0715; found 621.0711.

Crystals suitable for X-ray analysis (identified as **ReAlkyne**, C₂₄H₁₃N₆O₃Re) were obtained by liquid-liquid diffusion of Et₂O into a CH₂Cl₂ solution of the complex.

ReBn

To a stirring solution of **ReAlkyne** (70 mg, 0.111 mmol) and benzyl azide **5** (15 mg, 0.111 mmol) in DMF/H₂O (8:2, 10 mL) was added a previously homogenized (using sonication) solution of sodium ascorbate (5 mg, 0.022 mmol) and CuSO₄·5H₂O (5 mg, 0.060 mmol) in DMF/H₂O (1:6, 1.2 mL) and stirring was maintained at ambient temperature for 24 h. The reaction mixture was then concentrated under reduced pressure and resuspended in a stirring solution of CH₂Cl₂/conc. NH₄OH (1:1, 20 mL) at ambient temperature for 24 h. The mixture was partitioned in a separatory funnel and washed with H₂O (3 × 20 mL). The organic phases were combined and dried over Na₂SO₄, filtered and concentrated under reduced pressure. The title complex was purified from the crude material by column chromatography on Al₂O₃ using CH₂Cl₂/EtOAc (8:2) to give **9** as a yellow powder (70 mg, 84%). ν_{\max} (IR)/cm⁻¹, CH₂Cl₂: 2028 s (CO, A'(1)), 1922 s br (CO, A'(2)/A''). ¹H NMR (400 MHz, CDCl₃): δ 5.42 (2H, s, CN₄-C₆H₄-N₃C₂H-CH₂-C₆H₅), 7.18–7.21 (2H, m, CN₄-C₆H₄-N₃C₂H-CH₂-C₆H₅), 7.26–7.28 (3H, m, CN₄-C₆H₄-N₃C₂H-CH₂-C₆H₅), 7.54 (3H, m, CN₄-C₆H₄-N₃C₂H-CH₂-C₆H₅ and CN₄-C₆H₄-N₃C₂H-CH₂-C₆H₅), 7.71–7.74 (4H, m, phen and CN₄-C₆H₄-N₃C₂H-CH₂-C₆H₅), 7.83 (2H, s, phen), 8.41 (2H, d, $J = 8.4$ Hz, phen), 9.38 (2H, d, $J = 6.4$ Hz, phen); ¹³C NMR (100 MHz, CD₃CN): 196.4, 195.3, 163.5, 155.1, 149.8, 148.4, 140.4,

132.8, 131.8, 131.7, 131.6, 130.4, 130.2, 128.7, 128.6, 127.6, 127.4, 126.6, 122.7, 57.3. ESI-MS, m/z for $C_{31}H_{20}N_9O_3Re$ $[M + H]^+$ calc. 757.1; found 758.1.

Crystals suitable for X-ray analysis (identified as **ReBn**·CH₂Cl₂, C₃₂H₂₅Cl₂N₉O₃Re) were obtained by liquid-liquid diffusion of Et₂O into a solution of the complex in CH₂Cl₂.

General procedure for glycosylation reactions

To a stirred solution of per-*O*-acetyl saccharide (1.0 equiv.) in anhydrous CH₂Cl₂ (0.3 M) at 0 °C, under an inert atmosphere, was added slowly BF₃O·(C₂H₅)₂ (6.0 equiv.), followed by 2-bromoethanol (3.5 equiv.). The reaction was slowly warmed to ambient temperature and stirring was maintained for 16 h. The reaction was quenched with sat. NaHCO₃ and the solution was transferred to a separatory funnel. The phases were separated, and the organic portion was washed with H₂O (2 × 25 mL) and brine (25 mL), dried (Na₂SO₄), filtered and concentrated *in vacuo*. Purification of the crude material is outlined below.

2-Bromoethyl 2,3,4,6-tetra-*O*-acetyl-β-D-glucoside (7) was obtained from β-D-glucose pentaacetate **6** (3.07 g, 7.85 mmol) after recrystallization from hot EtOH to give the title compound (1.22 g, 34%) as a fluffy white solid. m.p 114–115 °C. (lit. 119–120 °C).³¹ ¹H NMR (500 MHz, CDCl₃) δ 5.22 (1H, app. t, J = 9.8 Hz, H3), 5.09 (1H, app. t, J = 9.8 Hz, H4), 5.02 (1H, dd, J = 9.8, 8.0 Hz, H2), 4.57 (1H, d, J = 8.0 Hz, H1), 4.26 (1H, dd, J = 12.0, 4.8 Hz, H6), 4.18–4.13 (2H, m, OCH₂, H6), 3.81 (1H, ddd, J = 13.5, 7.5, 6.0 Hz, OCH₂), 3.71 (1H, dd, J = 9.8, 4.8, 2.5 Hz, H5), 3.48–3.44 (2H, m, CH₂Br), 2.09 (3H, s, CH₃), 2.07 (3H, s, CH₃), 2.03 (3H, s, CH₃), 2.01 (3H, s, CH₃). ¹³C NMR (125 MHz, CDCl₃) δ 170.8, 170.4, 169.6, 169.5, 101.2, 72.7, 72.1, 71.2, 70.0, 68.5, 62.0, 30.0, 20.90, 20.89, 20.8, 20.7. HRMS (ESI, m/z) for C₁₆H₂₃⁷⁹BrO₁₀ $[M + Na]^+$ calc. 477.0367; found 477.0366.

2-Bromoethyl 2,3,4,6-tetra-*O*-acetyl- β -D-galactopyranose (11) was obtained from β -D-galactose pentaacetate **10** (6.08 g, 15.58 mmol) after purification using column chromatography (10% EtOAc in CH₂Cl₂), followed by recrystallization from hot CH₂Cl₂ as a white crystalline solid (1.16 g, 24%). R_f = 0.44 (10% EtOAc in CH₂Cl₂). m.p 111–112 °C. (lit. 111 °C).³² ¹H NMR (500 MHz, CDCl₃) δ 5.40 (1H, dd, J = 3.5, 1.0 Hz, H4), 5.23 (1H, dd, J = 10.5, 8.0 Hz, H3), 5.02 (1H, dd, J = 10.5, 3.2 Hz, H2), 4.54 (1H, d, J = 3.2 Hz, H1), 4.20–4.16 (3H, m, H6, OCH₂), 3.91 (1H, app. t, J = 6.6 Hz, H5), 3.82 (1H, ddd, J = 13.5, 7.5, 6.0 Hz, OCH₂), 3.48–3.47 (2H, m, CH₂Br), 2.16 (3H, s, CH₃), 2.09 (3H, s, CH₃), 2.06 (3H, s, CH₃), 1.99 (3H, s, CH₃). ¹³C NMR (125 MHz, CDCl₃) δ 170.6, 170.4, 170.3, 169.7, 101.7, 71.0, 70.9, 69.9, 68.7, 67.1, 61.4, 30.1, 21.0, 20.83, 20.81, 20.7. HRMS (ESI, m/z) for C₁₆H₂₃⁷⁹BrO₁₀ [M+Na]⁺ calc. 477.0367; found 477.0364.

2-Bromoethyl 2,3,4,6-*O*-acetyl- α -D-mannopyranoside (15) was obtained from α -D-mannose pentaacetate **14** (3.065 g, 7.85 mmol) after recrystallization from hot EtOH as fine white crystals (1.66 g, 47%). m.p 116–118 °C. (lit. 115.1–117.2 °C).³³ ¹H NMR (500 MHz, CDCl₃) δ 5.86 (1H, dd, J = 10.1, 3.4 Hz, H3), 5.30–5.26 (2H, m, H2, H4), 4.87 (1H, d, J = 1.6 Hz, H1), 4.26 (1H, dd, J = 12.7, 5.9 Hz, H6), 4.14–4.11 (2H, m, H5, H6), 3.97 (1H, app. dt, J = 11.2, 6.1 Hz, OCH₂), 3.88 (1H, app. dt, J = 11.2, 6.1 Hz, OCH₂), 3.51 (2H, app. t, J = 6.1 Hz, CH₂Br), 2.15 (3H, s, CH₃), 2.10 (3H, s, CH₃), 2.04 (3H, s, CH₃), 1.99 (3H, s, CH₃). ¹³C NMR (125 MHz, CDCl₃) δ 170.7, 170.1, 170.0, 169.8, 97.8, 69.4, 69.0, 68.5, 66.1, 66.0, 62.4, 29.7, 20.9, 20.79, 20.75, 20.7. HRMS (ESI, m/z) for C₁₆H₂₃⁷⁹BrO₁₀ [M + Na]⁺ calc. 477.0367; found 477.0364.

2,3,6-Tetra-*O*-acetyl-4-*O*-(2,3,4,6-tetra-*O*-acetyl- α -D-glucopyranosyl)-1-*O*-(2-bromoethyl)- β -D-glucopyranoside (19) was obtained from β -D-maltose octaacetate **18** (5.120 g, 7.55 mmol) after purification using column chromatography (20% EtOAc in CH₂Cl₂) as a colorless oil

(3.567 g, 64%). $R_f = 0.52$ (20% EtOAc in CH_2Cl_2). m.p 71–73 °C. ^1H NMR (500 MHz, CDCl_3) δ 5.41 (1H, d, $J = 4.0$ Hz, H1), 5.35 (1H, app. t, $J = 9.9$ Hz, H3), 5.26 (1H, app. t, $J = 9.1$ Hz, H4'), 5.05 (1H, app. t, $J = 9.9$ Hz, H4), 4.87–4.82 (2H, m, H2, H2'), 4.59 (1H, d, $J = 7.4$ Hz, H1'), 4.49 (1H, dd, $J = 12.1, 2.7$ Hz, H6'), 4.26–4.20 (2H, m, H6', H6), 4.12 (1H, ddd, $J = 11.2, 9.0, 5.7$ Hz, OCH_2), 4.06–3.94 (3H, m, H6, H5, H3'), 3.81 (1H, ddd, $J = 11.2, 7.2, 7.2$ Hz, OCH_2), 3.69 (1H, ddd, $J = 9.6, 4.3, 2.7$ Hz, H5'), 3.46–3.42 (2H, m, CH_2Br), 2.14 (3H, s, CH_3), 2.10 (3H, s, CH_3), 2.04 (6H, s, $2 \times \text{CH}_3$), 2.02 (3H, s, CH_3), 2.00 (3H, s, CH_3), 1.99 (3H, s, CH_3). ^{13}C NMR (125 MHz, CDCl_3) δ 170.7 ($2 \times \text{C}$), 170.6, 170.3, 170.1, 169.8, 169.6, 100.6, 95.7, 75.3, 72.7, 72.4, 72.0, 70.1, 69.9, 69.5, 68.7, 68.1, 62.8, 61.6, 30.0, 21.04, 20.99, 20.9, 20.84, 20.76, 20.73, 20.72. HRMS (ESI, m/z) for $\text{C}_{28}\text{H}_{39}^{79}\text{BrO}_{18}$ $[\text{M} + \text{Na}]^+$ calc. 765.1212; found 765.1209.

General procedure for azidation reactions

Adapted from a previously published method,³⁴ a mixture of 2-bromoethyl acetylated saccharide (1.0 equiv.) and NaN_3 (3.0 equiv.) in DMF (0.1M) was stirred at 100 °C for 1.5 h under an inert atmosphere. The reaction mixture was diluted with EtOAc (20 mL) and transferred to a separatory funnel and washed with H_2O (4×15 mL), brine (15 mL), dried with Na_2SO_4 , filtered and concentrated under reduced pressure to give the desired product.

2-Azidoethyl 2,3,4,6-tetra-*O*-acetyl- β -D-glucopyranoside (8) was obtained from bromo 7 (1.21 g, 2.66 mmol) as a white solid (890 mg, 80%). m.p 118–119 °C. (lit. 115.7–116.7 °C).³⁴ ^1H NMR (500 MHz, CDCl_3) δ 5.20 (1H, app. t, $J = 9.5$ Hz, H3), 5.08 (1H, app. t, $J = 10.0$ Hz, H4), 5.01 (1H, dd, $J = 9.5, 8.0$ Hz, H2), 4.58 (1H, d, $J = 8.0$ Hz, H1), 4.24 (1H, dd, $J = 12.4, 4.7$ Hz, H6), 4.15 (1H, dd, $J = 12.4, 2.5$ Hz, H6), 4.02 (1H, ddd, $J = 10.5, 4.5, 3.5$ Hz, OCH_2), 3.72–3.65 (2H, m, OCH_2 , H5), 3.49 (1H, ddd, $J = 13.4, 8.4, 3.5$ Hz, CH_2N_3), 3.27 (1H, ddd, $J = 13.4, 4.5, 3.0$

Hz CH₂N₃), 2.07 (3H, s, CH₃), 2.04 (3H, s, CH₃), 2.01, (3H, s, CH₃), 1.99 (3H, s, CH₃). ¹³C NMR (125 MHz, CDCl₃) δ 170.8, 170.4, 169.52, 169.51, 100.8, 72.9, 72.0, 71.2, 68.7, 68.4, 61.9, 50.6, 20.84, 20.79, 20.74, 20.73. HRMS (ESI, *m/z*) for C₁₆H₂₃N₃O₁₀ [M + Na]⁺ calc. 440.1276; found 440.1275.

2-Azidoethyl 2,3,4,6-tetra-*O*-acetyl-β-D-galactopyranoside (12) was obtained from bromo **11** (1.16 g, 2.54 mmol) as a colourless viscous oil (1.06 g, 99%). ¹H NMR (500 MHz, CDCl₃) δ 5.32 (1H, dd, *J* = 3.5, 1.0 Hz, H₄), 5.15 (1H, dd, *J* = 10.5, 8.0 Hz, H₂), 4.95 (1H, dd, *J* = 10.5, 3.5 Hz, H₃), 4.50 (1H, d, *J* = 8.0 Hz, H₁), 4.04–4.02 (1H, m, OCH₂), 3.97 (1H, ddd, *J* = 11.0, 4.7, 3.5 Hz, OCH₂), 3.87 (1H, dd, *J* = 6.5, 1.0 Hz, H₅), 3.63 (1H, ddd, *J* = 11.0, 8.2, 3.3 Hz, OCH₂), 3.43 (1H, ddd, *J* = 13.5, 8.2, 3.5 Hz, CH₂N₃), 3.25 (1H, ddd, *J* = 13.5, 4.7, 3.3 Hz, CH₂N₃), 2.08 (3H, s, CH₃), 1.99 (3H, s, CH₃), 1.97 (3H, s, CH₃), 1.91 (3H, s, CH₃). ¹³C NMR (125 MHz, CDCl₃) δ 170.3, 170.1, 170.0, 169.4, 101.0, 70.8, 70.7, 68.5, 68.3, 67.0, 61.2, 50.5, 20.7, 20.58, 20.57, 20.5. HRMS (ESI, *m/z*) for C₁₆H₂₃N₃O₁₀ [M + Na]⁺ calc. 440.1276; found 440.1279.

2-Azidoethyl 2,3,4,6-*O*-acetyl-α-D-mannopyranoside (16) was obtained from bromo **15** (963 mg, 2.12 mmol) as a white waxy solid (711 mg, 80%). m.p 80–82 °C. (lit. 81.8–82.1 °C).³³ ¹H NMR (500 MHz, CDCl₃) δ 5.36 (1H, dd, *J* = 10.0, 3.5 Hz, H₃), 5.32–5.28 (2H, m, H₂, H₄), 4.87 (1H, d, *J* = 1.5 Hz, H₁), 4.29 (1H, dd, *J* = 12.3, 5.5 Hz, H₆), 4.13 (1H, dd, *J* = 12.3, 2.3 Hz, H₆), 4.05 (1H, ddd, *J* = 10.0, 5.5, 2.3 Hz, H₅), 3.86 (1H, ddd, *J* = 10.2, 6.4, 3.7 Hz, OCH₂), 3.66 (1H, ddd, *J* = 10.2, 6.4, 3.7 Hz, OCH₂), 3.52–3.42 (2H, m, CH₂N₃), 2.16 (3H, s, CH₃), 2.10 (3H, s, CH₃), 2.05 (3H, s, CH₃), 2.00 (3H, s, CH₃). ¹³C NMR (125 MHz, CDCl₃) δ 170.8, 170.2, 170.0, 169.9, 97.9, 69.5, 69.0, 67.2, 66.1, 62.6, 50.5, 21.0, 20.9, 20.82, 20.77. HRMS (ESI, *m/z*) for C₁₆H₂₃N₃O₁₀ [M + Na]⁺ calc. 440.1276; found 440.1272.

2,3,6-Tetra-*O*-acetyl-4-*O*-(2,3,4,6-tetra-*O*-acetyl- α -D-glucopyranosyl)-1-*O*-(2-azidoethyl)- β -D-glucopyranoside (20) was obtained from bromo **19** (227 mg, 0.305 mmol) as a white waxy solid (177 mg, 82%). m.p 96–98 °C. (lit. 92.9–93.6 °C).³⁴ ¹H NMR (500 MHz, CDCl₃) δ 5.41 (1H, d, J = 4.0 Hz, H1), 5.36 (1H, app. t, J = 10.0 Hz, H3), 5.25 (1H, app. t, J = 9.2 Hz, H4'), 5.05 (1H, app. t, J = 10.0 Hz, H4), 4.87–4.83 (2H, m, H2, H2'), 4.61 (1H, d, J = 7.9 Hz, H1'), 4.52 (1H, dd, J = 12.2, 2.5 Hz, H6'), 4.26–4.19 (2H, m, H6, H6'), 4.06–3.94 (4H, m, H5, H6, H3', OCH₂), 3.72–3.67 (2H, m, H5', OCH₂), 3.47 (1H, ddd, J = 13.4, 8.3, 3.3 Hz, CH₂N₃), 3.26 (1H, ddd, J = 13.4, 8.1, 4.1 Hz, CH₂N₃), 2.14 (3H, s, CH₃), 2.10 (3H, s, CH₃), 2.04–2.00 (15H, m, 4 \times CH₃). ¹³C NMR (125 MHz, CDCl₃) δ 170.7, 170.6, 170.4, 170.1, 169.8, 169.5, 100.3, 95.7, 75.5, 72.7, 72.4, 72.1, 70.1, 69.5, 68.9, 68.6, 68.1, 62.7, 61.6, 50.6, 21.04, 20.98, 20.83, 20.81, 20.73, 20.71. HRMS(ESI, m/z) C₂₈H₃₉N₃O₁₈ [M + Na]⁺ calc. 728.2121; found 728.2107.

General procedure for deacetylation reactions

Adapted from a previously published method,³⁵ a solution of 2-azidoethyl acetylated saccharide (1.0 equiv.) in MeOH (0.2 M) was added NaOMe (5.0 equiv. unless otherwise stated) and stirred for 24 h at ambient temperature. The pH of the solution was adjusted to pH = 6 by addition of Amberlite® IR120 H⁺ cation exchange resin. The suspension was filtered and the filtrate was collected and concentrated under reduced pressure to give the desired product.

2-Azidoethyl-*O*- β -D-glucopyranoside (9) was obtained from tetraacetate **8** (146 mg, 0.350 mmol) as a colourless oil (86 mg, 98%). ¹H NMR (500 MHz, CD₃OD) δ 4.31 (1H, d, J = 7.8 Hz, H1), 4.03 (1H, ddd, J = 10.6, 5.1, 5.1 Hz, OCH₂), 3.88 (1H, dd, J = 11.6, 1.1 Hz, H6), 3.75 (1H, ddd, J = 10.6, 5.1, 5.1 Hz, OCH₂), 3.67 (1H, dd, J = 11.6, 5.4 Hz, H6), 3.47 (2H, app. t, J = 5.1 Hz, CH₂N₃), 3.37–3.27 (3H, m, H3, H4, H5), 3.20 (1H, dd, J = 9.1, 7.8 Hz, H2). ¹³C NMR

(125 MHz, CD₃OD) δ 104.3, 77.9, 77.8, 75.0, 71.5, 69.6, 62.6, 52.0. HRMS (ESI, m/z) for C₈H₁₅N₃O₆ [M+Na]⁺ calc. 272.0853; found 272.0852.

2-Azidoethyl-*O*- β -D-galactopyranoside (13) was obtained from tetraacetate **12** (298 mg, 0.714 mmol) as a colourless oil (155 mg, 87%). ¹H NMR (500 MHz, CD₃OD) δ 4.23 (1H, d, J = 7.5 Hz, H1), 4.03 (1H, ddd, J = 10.7, 5.1, 5.1 Hz, OCH₂), 3.80 (1H, dd, J = 3.0, 0.5 Hz, H4), 3.75–3.67 (3H, m, OCH₂, H6), 3.52–3.43 (5H, m, CH₂N₃, H2, H3, H5). ¹³C NMR (125 MHz, CD₃OD) δ 105.0, 76.7, 74.9, 72.4, 70.2, 69.2, 62.4, 52.0. HRMS (ESI, m/z) for C₈H₁₅N₃O₆ [M+Na]⁺ calc. 272.0853; found 272.0854.

2-Azidoethyl-*O*- α -D-mannopyranoside (17) was obtained from tetraacetate **16** (135 mg, 0.323 mmol) as a white solid (78 mg, 98%). m.p: 80–82 °C (lit. 142 °C).³⁵ ¹H NMR (500 MHz, CD₃OD) δ 4.82 (1H, d, J = 1.3 Hz, H1), 3.94–3.90 (1H, m, OCH₂), 3.86–3.83 (2H, m, H3, H6), 3.74–3.70 (2H, m, H2, H6), 3.65–3.55 (3H, m, OCH₂, H4, H5), 3.43 (2H, app. t, J = 5.0 Hz, CH₂N₃). ¹³C NMR (125 MHz, CD₃OD) δ 101.8, 74.9, 72.4, 72.0, 68.5, 67.7, 62.9, 51.7. HRMS (ESI, m/z) for C₈H₁₅N₃O₆ [M + Na]⁺ calc. 272.0853; found 272.0852.

2-Azidoethyl-*O*- β -D-maltopyranoside (21) was obtained from heptaacetate **20** (100 mg, 0.142 mmol) using 6.0 equivalents of NaOMe, as a white solid (58 mg, 99%). m.p 95–171 °C (slow decomposition). ¹H NMR (500 MHz, CD₃OD) δ 5.16 (1H, d, J = 3.8 Hz, H1), 4.33 (1H, d, J = 7.8 Hz, H1'), 4.02 (1H, ddd, J = 10.7, 5.2, 5.2 Hz, OCH₂), 3.90 (1H, dd, J = 12.2, 1.9 Hz, H6'), 3.83–3.79 (2H, m, H6, H6'), 3.74 (1H, ddd, J = 10.7, 5.2, 5.2 Hz, OCH₂), 3.70–3.59 (4H, m, H3, H5, H6, H2'), 3.54 (1H, app. t, J = 9.5 Hz, H4'), 3.48–3.43 (3H, m, H2, CH₂N₃), 3.39 (1H, ddd, J = 9.6, 4.7, 1.9 Hz, H5'), 3.29–3.24 (2H, m, H4, H3'). ¹³C NMR (125 MHz, CD₃OD) δ 104.4, 102.9, 81.2, 77.8, 76.7, 75.1, 74.8, 74.7, 74.2, 71.5, 69.4, 62.7, 62.2, 52.0. HRMS (ESI, m/z) for C₁₄H₂₅N₃O₁₁ [M + Na]⁺ calc. 434.1381; found 434.1380.

General procedure for CuACC reactions

To a stirred solution of **ReAlkyne** (1.0 equiv.) and azide (as specified) in DMF/H₂O (4:1) was added a previously homogenized (using sonication) solution of sodium ascorbate (1.7 equiv.) and CuSO₄·5H₂O (0.5 equiv.) in DMF/H₂O (1:6, 1.2 mL). The reaction was stirred at ambient temperature for 24–72 h until the **ReAlkyne** material was consumed, as evidenced by ESI-MS. The reaction mixture was concentrated under a stream of N₂ to give a green solid. The crude material was suspended in sat. NaHCO₃ (8 mL), centrifuged for 5 min at 7500 RPM and the supernatant was discarded. This process was repeated using sat. NaHCO₃, H₂O and CH₂Cl₂ three times each. The resulting dark yellow solid was dissolved in anhydrous MeOH (5 mL), filtered through a syringe filter (0.45 µm nylon) and concentrated *in vacuo* to give the desired product.

ReGlucose was obtained from **ReAlkyne** (30 mg, 0.048 mmol) and azide **9** (24 mg, 0.096 mmol) as a yellow solid (40 mg, 96%). m.p: 203–240 °C (slow decomposition). ¹H NMR (500 MHz, CD₃OD) δ 9.57 (2H, dd, *J* = 5.2, 1.3 Hz, H2, H9), 8.80 (2H, dd, *J* = 8.3, 1.3 Hz, H4, H7), 8.41 (1H, s, triazole-H), 8.15 (2H, s, H5, H6), 8.01 (2H, dd, *J* = 8.3, 5.2 Hz, H3, H8), 7.67 (2H, d, *J* = 8.4 Hz, *o*-ArH), 7.57 (2H, d, *J* = 8.4 Hz, *m*-ArH), 4.67–4.64 (2H, m, NCH₂), 4.33 (1H, d, *J* = 7.8 Hz, H1'), 4.29–4.25 (1H, m, OCH₂), 4.04–4.00 (1H, m, OCH₂), 3.85 (1H, dd, *J* = 12.1, 1.5 Hz, H6'), 3.66–3.63 (1H, m, H6'), 3.34–3.26 (3H, m, H3', H4', H5'), 3.20 (1H, dd, *J* = 9.1, 7.8 Hz, H2'). ¹³C NMR (125 MHz, CD₃OD) δ 197.6 (2 × C=O), 194.6 (C=O), 163.8 (tetrazole C), 155.3 (2 × C, C2, C9), 148.6 (2 × C, C10a, C10b), 148.0 (triazole C), 140.6 (2 × C, C4, C7), 132.3 (*p*-Ar), 132.1 (2 × C, C4a, C6a), 129.7 (*i*-Ar), 128.9 (2 × C, C5, C6), 127.6 (2 × C, *o*-Ar), 127.4 (2 × C, C3, C8), 126.7 (2 × C, *m*-Ar), 123.6 (Triazole CH), 104.5 (C1'), 78.1 (C3'), 78.0 (C5'), 75.0 (C2'), 71.5 (C4'), 69.1 (OCH₂), 62.7 (C6'), 51.7 (NCH₂). HRMS (ESI, *m/z*) for C₃₂H₂₈N₉O₉Re [M

+ H]⁺ calc. 870.1640; found 870.1644. Anal. RP-HPLC Method A: *t*_R 11.37 min, purity >97%; Method B: *t*_R 10.11 min, purity >96%.

ReGalactose was obtained from **ReAlkyne** (29 mg, 0.047 mmol) and azide **13** (23 mg, 0.092 mmol) as a yellow solid (36 mg, 87%). m.p: 200–240 °C (slow decomposition). ¹H NMR (500 MHz, CD₃OD) δ 9.57 (2H, dd, *J* = 6.2, 1.3 Hz, H2, H9), 8.82 (2H, dd, *J* = 8.4, 1.3 Hz, H4, H7), 8.43 (1H, s, triazole-H), 8.16 (2H, s, H5, H6), 8.03 (2H, dd, *J* = 8.4, 6.2 Hz, H3, H8), 7.69 (2H, d, *J* = 8.4 Hz, *m*-ArH), 7.57 (2H, d, *J* = 8.4 Hz, *o*-ArH), 4.67 (2H, app. t, *J* = 4.9 Hz, NCH₂), 4.29–4.25 (2H, m, H1', OCH₂), 4.04–4.00 (1H, m, OCH₂), 3.82 (1H, d, *J* = 2.8 Hz, H4'), 3.76–3.68 (2H, m, H6'), 3.55–3.51 (2H, m, H2'', H5'), 3.45 (1H, dd, *J* = 8.8, 2.8 Hz, H3'). ¹³C NMR (125 MHz, CD₃OD) δ 197.8 (2 × C=O), 194.5 (C=O), 163.8 (tetrazole C), 155.3 (2 × C, C2, C9), 148.6 (2 × C, C10a, C10b), 148.0 (triazole C), 140.6 (2 × C, C4, C7), 132.3 (*p*-Ar), 132.2 (2 × C, C4a, C6a), 129.7 (*i*-Ar), 128.9 (2 × C, C5, C6), 127.6 (2 × C, *o*-Ar), 127.5 (2 × C, C3, C8), 126.7 (2 × C, *m*-Ar), 123.7 (triazole CH), 105.3 (C1'), 76.8 (C2'), 74.9 (C3'), 72.4 (C5'), 70.3 (C4'), 69.2 (OCH₂), 62.6 (C6'), 51.8 (NCH₂). HRMS (ESI, *m/z*) for C₃₂H₂₈N₉O₉Re [M + H]⁺ calc. 870.1640; found 870.1649. Anal. RP-HPLC Method A: *t*_R 11.41 min, purity >95%; Method B: *t*_R 10.13 min, purity >95%.

ReMannose was obtained from **ReAlkyne** (39 mg, 0.063 mmol) and azide **17** (188 mg, 0.754 mmol) as a yellow solid (29 mg, 53%). m.p 205–240 °C (slow decomposition). ¹H NMR (500 MHz, CD₃OD) δ 9.57 (2H, dd, *J* = 5.2, 1.3 Hz, H2, H9), 8.81 (2H, dd, *J* = 8.3, 1.3 Hz, H4, H7), 8.29 (1H, s, H15), 8.16 (2H, s, H5, H6), 8.03 (2H, dd, *J* = 8.3, 5.2 Hz, H3, H8), 7.69 (2H, d, *J* = 8.4 Hz, *m*-ArH), 7.59 (2H, d, *J* = 8.4 Hz, *o*-ArH), 4.74 (1H, d, *J* = 1.4 Hz, H1'), 4.69–4.59 (2H, m, NCH₂), 4.17–4.13 (1H, m, OCH₂), 3.93–3.87 (1H, m, OCH₂), 3.77–3.73 (2H, m, H3', H6'), 3.64–3.54 (3H, m, H2', H4', H6'), 3.31–3.28 (1H, m, H5'). ¹³C NMR (125 MHz, CD₃OD) δ 197.6 (2 ×

C=O), 194.5 (C=O), 163.8 (C11), 155.3 (2 × C, C2, C9), 148.6 (2 × C, C10a, C10b), 148.2 (C14), 140.6 (2 × C, C4, C7), 132.1 (3 × C, C4a, C6a, C13), 129.8 (C12), 128.9 (2 × C, C5, C6), 127.6 (2 × C, *o*-Ar), 127.4 (2 × C, C3, C8), 126.8 (2 × C, *m*-Ar), 123.0 (C15), 101.8 (C1'), 75.0 (C5'), 72.4 (C2'), 71.9 (C3'), 68.3 (C4'), 66.8 (OCH₂), 62.8 (C6'), 51.4 (NCH₂). HRMS (ESI, *m/z*) for C₃₂H₂₈N₉O₉Re [M + H]⁺ calc. 870.1640; found 870.1638. Anal. RP-HPLC Method A: *t_R* 11.40 min, purity >91%; Method B: *t_R* 10.16 min, purity >90%.

ReMaltose was obtained from **ReAlkyne** (20 mg, 0.032 mmol) and azide **21** (40 mg, 0.097 mmol) as a yellow solid (19 mg, 57%). m.p: 198–240 °C (slow decomposition). ¹H NMR (500 MHz, CD₃OD) δ 9.57 (2H, d, *J* = 5.1, 1.3 Hz, H4, H7), 8.80 (2H, d, *J* = 8.2 Hz, H2, H9), 8.41 (1H, s, triazole-H), 8.15 (2H, s, H5, H6), 8.02 (2H, dd, *J* = 8.2, 5.1 Hz, H3, H8), 7.68 (2H, d, *J* = 8.4 Hz, *m*-ArH), 7.57 (2H, d, *J* = 8.4 Hz, *o*-ArH), 5.15 (1H, d, *J* = 3.8 Hz, H1''), 4.67–4.64 (2H, m, NCH₂), 4.35 (1H, d, *J* = 7.8 Hz, H1'), 4.28–4.24 (1H, m, OCH₂CH₂N), 4.04–4.00 (1H, m, OCH₂CH₂N), 3.89–3.77 (3H, m, H6', H6''), 3.69–3.58 (4H, m, H3', H6', H2'', H4''), 3.52 (1H, app. t, *J* = 9.4 Hz, H5''), 3.44 (1H, dd, *J* = 9.7, 3.7 Hz, H2'), 3.40–3.37 (1H, m, H3''), 3.28–3.23 (2H, m, H4', H5'). ¹³C NMR (125 MHz, CD₃OD) δ 197.6, 194.5, 163.7 (tetrazole), 155.3 (2 × C, C4, C7), 148.6 (2 × C, C10a, C10b), 148.0 (triazole C), 140.6 (2 × C, C2, C9), 132.3 (*p*-Ar), 132.1 (2 × C, C4a, C6a), 129.7 (*i*-Ar), 128.9 (2 × C, C5, C6), 127.6 (2 × C, *o*-Ar), 127.4 (2 × C, C3, C8), 126.7 (2 × C, *m*-Ar), 123.7 (triazole CH), 104.5 (C1'), 102.9 (C1''), 81.1 (C5''), 77.7 (C4''), 76.7 (C3''), 75.0 (C3'), 74.8 (C2''), 74.5 (C5') 74.1 (C2'), 71.5 (C4'), 69.2 (OCH₂CH₂N), 62.7 (C6'), 62.1 (C6''), 51.7 (NCH₂). HRMS (ESI, *m/z*) for C₃₈H₃₈N₉O₁₄Re [M+H]⁺ calc. 1032.2168; found 1032.2194. Anal. RP-HPLC Method A: *t_R* 11.24 min, purity >97%; Method B: *t_R* 9.88 min, purity >97%.

X-ray crystallography

Crystal data and collection details for **ReAlkyne** and **ReBn** are reported in supplementary information (**ESI Tables S1** and **S2**). The diffraction experiments were carried out on a Bruker APEX II diffractometer equipped with a CCD detector and using Mo-K α radiation. Data were corrected for Lorentz polarisation and absorption effects (empirical absorption correction SADABS). Structures were solved by direct methods and refined by full-matrix least-squares based on all data using F^2 .³⁶ H-atoms were placed in calculated positions, and refined isotropically using a riding model. All non-hydrogen atoms were refined with anisotropic displacement parameters.

Photophysical evaluation

Absorption spectra were recorded at room temperature using a CARY eclipse 50 scan UV-visible spectrophotometer (**Figure 3**). Emission spectra were collected on a CARY Eclipse fluorescence spectrometer (**Figure 3** and **ESI S14-S15**). The complexes were excited at the excitation maxima of 275 nm and at 405 nm (a wavelength analogous to the instrumentation used for live cell imaging), using a PMT detector voltage of 600 V and excitation/emission slit widths of 2.5 nm. The spectra for **Figure 3** and **ESI S14-S15** were recorded using a mixed aqueous solution of 1:1 MeOH/H₂O to ensure solubility. Suprasil quartz cuvettes of 1 cm path length at right angle detection were used for all experiments. pH titration measurements were performed using a pre-calibrated Orion Ross pH meter and were conducted at a constant ionic strength of 1×10^{-3} M using NaCl across a pH range of pH 4–8 at 275 nm excitation wavelength.

The determination of quantum yields and lifetimes (**Table 1**) was performed on an Edinburgh FLSP980-S2S2-stm spectrometer equipped with: i) a temperature-monitored cuvette holder; ii) 450 W Xenon arc lamp; iii) double excitation and emission monochromators; iv) a Peltier cooled Hamamatsu R928P photomultiplier tube (spectral range 200–870 nm). According to the approach described by Demas and Crosby,³⁷ luminescence quantum yields (Φ_{em}) were measured in optically

dilute solutions (O.D. < 0.1 at excitation wavelength) obtained from absorption spectra on a wavelength scale [nm] and compared to the reference emitter ([Ru(bipy)₃]Cl₂ (bipy = 2,2'-bipyridine; Φ_f = 0.04)).³⁸ Spectra were recorded in a 1% DMSO in H₂O solution to match the conditions used in live cell imaging and ensure complete dissolution was maintained. Emission lifetimes (τ) were determined with the time correlated single-photon counting technique (TCSPC), with the same Edinburgh FLSP980-S2S2-stm spectrometer, using a pulsed picosecond LED (EPLED/EPL 377 nm, FWHM < 800 ps). The goodness of fit was assessed by minimizing the reduced χ^2 function and by visual inspection of the weighted residuals. The solvents used for the preparation of the solutions for the photophysical investigations were of LR grade and the water was deionized. Experimental uncertainties are estimated to be $\pm 8\%$ for lifetime determinations, $\pm 20\%$ for quantum yields, ± 2 nm and ± 5 nm for absorption and emission peaks, respectively.

Lipophilicity determination

The *n*-octanol/H₂O partition coefficient (Log*D*) of the carbohydrate-appended Re(I) complexes was determined using the “shake-flask” method (**Table 2**).³⁹ Phosphate buffered saline (PBS) solution (200 mL, pH 7.4) and *n*-octanol (200 mL) were vortexed for 72 h in order to saturate both phases. After saturation, the two phases were separated by centrifugation (3000 rpm, 15 min). Carbohydrate-conjugated Re(I) complexes were prepared in DMSO (2000 ppm), 30 μ L of each solution was combined with saturated PBS solution (500 μ L) and saturated *n*-octanol (530 μ L) and mixed using a laboratory vortex for 10 min. The resulting emulsion was centrifuged (3000 rpm, 10 min) to separate the phases. The concentrations of each complex in the aqueous and organic phases were determined using UV-visible spectroscopy at 275 nm; log*D*_{7.4} was defined as the logarithm of the ratio of the concentrations of the complex in the organic and aqueous phase; the value reported is the mean of three separate determinations.

Cell culture

Rat embryonic cardiomyoblast-derived H9c2 cells were cultured in DMEM medium (#D6171, Sigma-Aldrich, USA), supplemented with 10% fetal bovine serum (FBS; #IVT3008403, In Vitro Technologies, Australia) and 2 mM L-glutamine (#25030-081, Gibco[®], USA). When cells reached ~80% confluence, cell culture media was aspirated, cells were washed with sterile PBS (#D8537, Sigma-Aldrich, USA) and then detached using TrypLE[™] Express (#12604-021, Gibco[®], USA). For staining, cells were seeded onto μ -Slide 8-well ibidi chambers (#80826.S, DKSH, Australia) at $\sim 2 \times 10^5$ cells/mL ($V = 300 \mu\text{L}$) and left overnight to adhere.

Staining and analysis of total cellular Re content by ICP-MS

The H9c2 cells, grown in T25 tissue flasks ($V = 11 \text{ mL}$) until 80–90% confluency for ~24 h, were incubated with the carbohydrate-conjugated Re(I) complexes ($1 \times 10^{-4} \text{ M}$) in a complete DMEM media at 37 °C under a 5% CO₂ for 4 h. The media was removed, and the cells were washed gently with PBS (3 \times 5 min). The cells were then detached using TrypLE[™] Express. A cell count was performed, before cell lysis was performed by syringe.

The cell lysate was desiccated in a dry block heater at 95 °C. The dry cell samples were then suspended in 36% HNO₃ (400 μL) and heated at 95 °C until dry to digest organic material and liberate Re from the sample, simplifying the matrix for ICP-MS analysis. The dry samples were then reconstituted in 2% HNO₃ (2.5 mL) and sonicated for 20 min to produce a clear solution. The samples were then filtered through a syringe filter cartridge with a pore diameter of 0.2 μm and analyzed for total Re using ICP-MS. Concentration values were corrected in respect to indium (In) as an internal standard at 10 ppb. Total Re determination was performed with an Agilent 8900x triple quad ICP-MS (QQQ-ICPMS), with no gas in the collision cell to improve sensitivity. For

quantitative determination, the most abundant isotopes of ^{185}Re and ^{115}In were analyzed. The analysis was performed against a calibration series, which was prepared from a multielement standard in 2% HNO_3 . The calibration series were as follows: 1, 5, 10, 20, 30, 50, 80, 100, 150, 200 and 500 ppb. A blank sample of the 2% HNO_3 solution was prepared as a negative control. Samples were run on an Agilent 8900x triple quad ICP-MS (QQQ-ICPMS). The instrument was tuned for matrix tolerance (1550W, 10mm sample depth, 1.09 L/min Ar carrier gas flow rate) and high sensitivity, while keeping oxides and doubly charged ions low ($<1.0\%\text{CeO/Ce}$ and $0.8\%\text{Ce}^{++}/\text{Ce}$, respectively).

Staining cells with the carbohydrate-conjugated Re(I) complexes

The H9c2 cells were incubated with **ReGlucose**, **ReGalactose**, **ReMannose** and **ReMaltose** at various 2×10^{-5} , 1×10^{-4} or 1.5×10^{-4} M, prepared in cell culture media containing 1% DMSO, for either 30 min or 24 h at 37 °C. Following incubation, cells were rinsed with cell culture media and imaged live, using confocal laser scanning microscope, supplemented with an Uno-Combined-Controller CO_2 microscope electric top stage incubation system.

The H9c2 cells, incubated for 24 h with **ReGlucose**, **ReGalactose** and **ReMannose** complexes at 1×10^{-4} M (1% DMSO in DMEM media), were counterstained for 1 min with Lyso-Tracker™ Red DND-99 (#L7528, Life Technologies, Australia) or 20 min with ER-Tracker™ Red (#E34250, Life Technologies, Australia). Cells, stained with **ReMaltose** (1.5×10^{-4} M) for 30 min, were rinsed and co-stained either with Lyso-Tracker™ Red DND-99 or ER-Tracker™ Red according to manufactures instructions.

Confocal laser scanning microscopy

All imaging experiments were conducted on a Nikon A1+ confocal laser scanning microscope, fitted with a LU-N4/LU-N4S 4-laser unit (403, 488, 561 and 640 nm), an A1-DUG GaAsP Multi

Detector Unit (two GaAsP PMTs and two standard PMTs) and a 32-channel spectral detector (Nikon). The carbohydrate-conjugated Re(I) complexes were excited using the 403 nm laser and emission was recorded across a range of 545–595 nm. The emission maxima of the complexes were at 565 nm. Both Lyso-Tracker™ Red DND-99 and ER-Tracker™ Red were imaged using the 561 nm laser. All images were collected using a 60 × oil immersion lens. Nikon NIS Element software was used to measure co-localisation of the Re(I) complexes with Lyso-Tracker™ and ER-Tracker™ using Pearson's coefficient. A minimum of 5 cells from three independent images were used to calculate and average the co-efficient for each combination of markers.

Cell viability assay

The H9c2 cells were grown at 1×10^4 cells/mL overnight in 96-well plates (100 μ L). Cells were incubated with the carbohydrate-conjugated Re(I) complexes (1×10^{-4} M) for 24 h at 37 °C and 5% CO₂. Negative controls were incubated with cell culture media, containing 1% DMSO. Following incubation, the media was removed, the cells were then washed with PBS (2 × 1 min), before being replaced with complete media. Resazurin cytotoxicity agent was added at 10% v/v and cells were incubated for further 3 h. The resazurin assay was then assessed on an EnSpire® multimode plate reader.

Results and Discussion

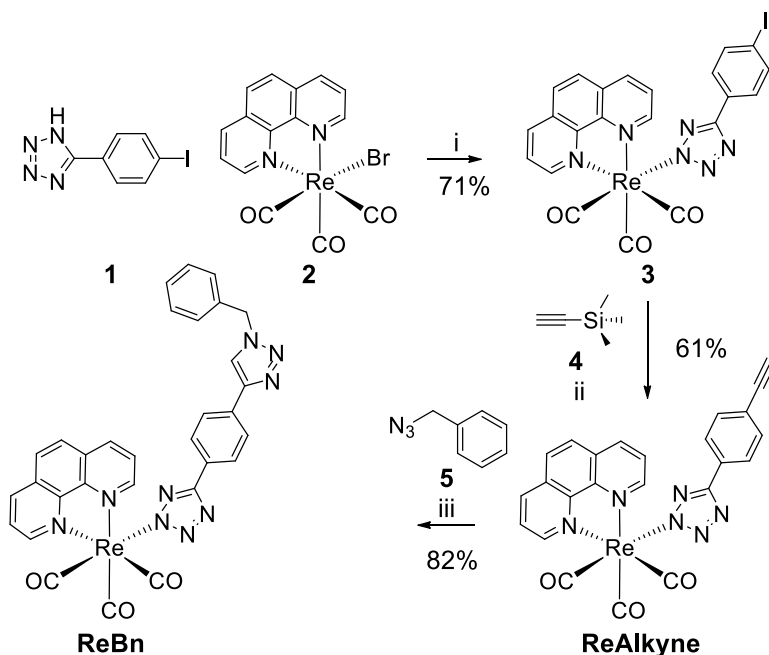
Synthesis and characterization

We first prepared the **ReAlkyne** complex and evaluated its ability to undergo Cu(I) Alkyne-Azide Cycloaddition (CuAAC) with benzyl azide as a model reaction for the bioconjugation with carbohydrate-based azides. Following this initial assessment, the same CuAAC strategy was applied for the preparation of the series of carbohydrate-conjugated Re(I) complexes. The

synthesis of **ReAlkyne** (**Scheme 1**) was achieved through a procedure based on the “chemistry on the complex” approach.⁴⁰

The precursory materials, 5-(4-iodophenyl)-1*H*-tetrazole **1** and *fac*-[Re(1,10-phenanthroline)(CO)₃(Br)] **2**, were synthesized following previously published procedures (see ESI for full synthetic details).²⁸⁻³⁰ Complex **3** was prepared through the coordination of **1** with the metal center of complex **2** in which the 5-(4-iodophenyl)tetrazolato anion fulfills the coordination sphere of the *fac*-[Re(CO)₃(phen)]⁺ fragment. **ReAlkyne** was then accessed by Sonogashira cross-coupling of **3** with **4**. The trimethylsilyl-protecting group was then cleaved to give **ReAlkyne** as a yellow solid in 61% yield. The ability of **ReAlkyne** to be used as a platform for bioconjugation was investigated by reacting benzyl azide **5** with **ReAlkyne** using CuAAC coupling conditions to give **ReBn**.

Scheme 1. Synthetic route for the ReAlkyne platform and ReBn.



Reagents and conditions: (i) Et₃N, EtOH/H₂O (3:1), 21 °C, 24 h; (ii) *cis*-[Pd(PPh₃)₂Cl₂], CuI, Et₃N, 74 THF, reflux, 24 h; (iii) **5**, CuSO₄·5H₂O, sodium ascorbate, DMF/H₂O (8:1), 21 °C, 24 h.

The solid-state structures of **ReAlkyne** and **ReBn** were confirmed using X-ray crystallography (**Figure 2**), which were in agreement with our previous reports detailing Re(I) tetrazolato or tetrazole complexes.⁴¹ The facial (*fac*) coordination geometry of the three CO ligands is evident and the aromatic rings of the ancillary tetrazolato ligand of each structure are almost coplanar, with the angles between the N₄C and C₆ rings determined as 6.8(10)° and 8.0(4)° for **ReAlkyne** (**Figure 2A**) and **ReBn** (**Figure 2B**), respectively. This arrangement is further extended to the triazole ring in the “click” conjugated complex **ReBn** (angle of 10.9(4)° between the N₃C₂ and C₆ rings); while the peripheral benzyl moiety appears to stand in a plane orthogonal with respect to the geometry of the tetrazolato-phenyl-triazole system (angle of 75.7(2)° between the N₃C₂ and benzyl rings) (**Figure 2B**). The determined bond lengths and angles that support the presented crystallographic structures of **ReAlkyne** and **ReBn** are provided as supplementary information (ESI Table S1 and S2).

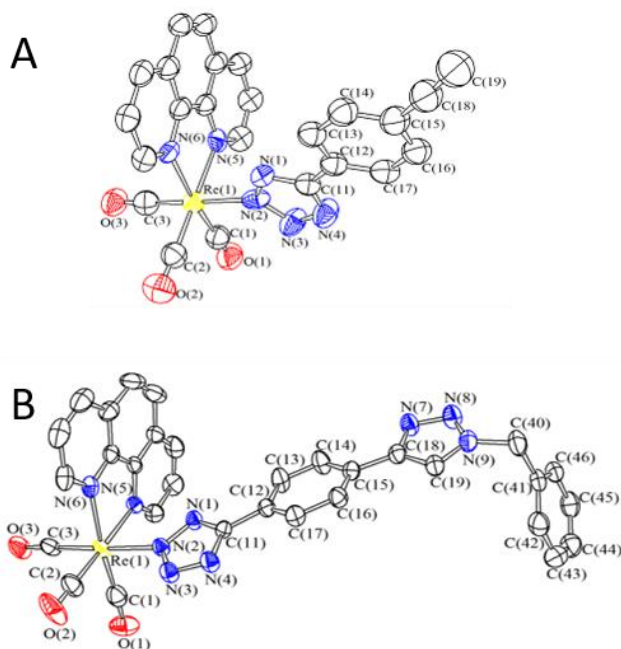
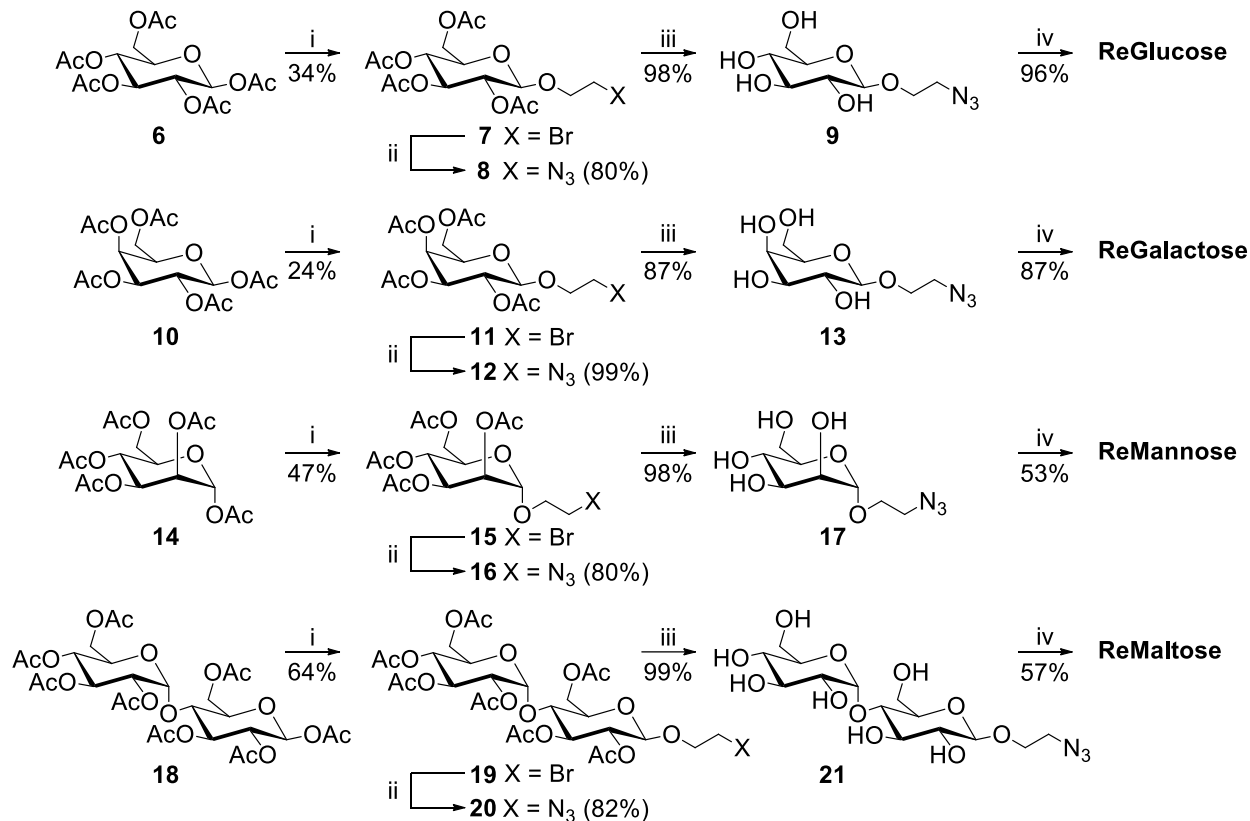


Figure 2. Molecular structure of (A) ReAlkyne and (B) ReBn with key atoms labelled. Displacement ellipsoids are presented at the 30% probability level and H-atoms are omitted for clarity.

With a procedure to bioconjugate **ReAlkyne** in-hand, our attention turned to the preparation of our targeted four carbohydrate (β -D-glucose, β -D-galactose, α -D-mannose and β -D-maltose) conjugated complexes; **ReGlucose**, **ReGalactose**, **ReMannose** and **ReMaltose** (**Figure 1**). These complexes were specifically designed to investigate the utility of the Re(I) platform for the exploration of cellular processes associated with the conjugated molecule; in this case, a simple carbohydrate. To synthesize the four targeted Re-carbohydrate complexes, the prerequisite azido carbohydrate building blocks were first prepared in an analogous fashion.

Scheme 2. Synthesis of -neutral carbohydrate-appended Re(I) complexes.



Reagents and conditions: (i) 2-bromoethanol, BF₃·(Et₂O)₂, CH₂Cl₂, 0–21 °C, 16 h; (ii) NaN₃, DMF, 100 °C, 1.5 h; (iii) NaOMe, MeOH, 21 °C, 24 h; (iv) **ReAlkyne**, CuSO₄·5H₂O, sodium ascorbate, 1:1 DMF/H₂O, 21 °C, 24 h.

Beginning from commercially available per-*O*-acetylated carbohydrate starting materials, installation of the 2-bromoethoxy linker to the anomeric carbon was achieved by Lewis acid-mediated glycosylation using BF₃·(Et₂O)₂ in CH₂Cl₂ under anhydrous conditions. Anomeric stereoselectivity was retained in each instance and purification was carried out by either crystallization (**7** and **11**), column chromatography (**19**) or a combination of both (**15**) to give spectroscopically pure materials, which matched previous literature reports.^{32, 42} Substitution using NaN₃ in *N,N*-dimethylformamide (DMF) at 100 °C gave the requisite azido carbohydrates in

excellent yields (80–99%), with only an extractive workup needed to isolate the pure material. Global deprotection of the acetyl groups was then performed using a methanolic NaOMe solution to reveal the carbohydrate hydroxyl groups in excellent yields (87–99%).⁴⁰ Each azido carbohydrate building block was then conjugated to **ReAlkyne** by CuAAC to afford the four targeted Re-conjugates; **ReGlucose**, **ReGalactose**, **ReMannose** and **ReMaltose** (**Figure 1**).

Photophysical characterization

The photophysical and spectral characteristics of each of the complexes were assessed to determine their suitability as agents for cellular imaging using confocal laser scanning microscopy. The excitation and emission profiles, emissive lifetime (τ) and quantum yield (ϕ) of the complexes were determined in a 1% DMSO in H₂O solution (**Table 1**).

Table 1. Photophysical properties (1% DMSO in H₂O).

Complex	Absorption	Emission		
	λ_{abs}	λ_{em}	τ_{aer}	ϕ_{aer}
	[nm] ($10^4 \epsilon$ [$\text{M}^{-1}\text{cm}^{-1}$])	[nm]	[ns]	
ReAlkyne^a	277 (4.62), 372 (0.360)	588	327	0.061
ReGlucose	273 (8.41), 373 (0.71)	584	300	0.034
ReGalactose	273 (9.96), 373 (0.83)	584	305	0.033
ReMannose	273 (9.74), 373 (0.81)	584	306	0.036
ReMaltose	273 (10.1), 373 (0.76)	584	308	0.041

ϕ_{aer} measured *versus* Ru(bpy)₃²⁺ in H₂O ($\phi_{\text{r}} = 0.040$);³⁸ (a) in CH₂Cl₂ solution (10^{-5} M)

Each complex exhibits an emissive lifetime of approximately 305 ns, with monoexponential decay. The lifetimes are similar to those previously reported for neutral [Re(CO)₃]⁺ polypyridyl tetrazolato complexes¹⁹ and glucose appended cationic Re(I) complexes.¹³ The emissive lifetimes of approximately 300 ns are also sufficient for signal resolution using time-gated imaging from endogenous fluorescent signals; for example, NAD(P)H emits within a brief window of only 0.4–6.0 ns.⁴³

The absorption spectra of each complex exhibit a prominent higher energy band at 273 nm (**Figure 3**), resulting from the spin-allowed ligand-centered π - π^* transition, while the broader and less intense band peaking in the 360–380 nm region is ascribed to metal-to-ligand charge transfer (MLCT) transitions. Activation of the MLCT manifold results in triplet state MLCT emission as a prominent band at 584 nm.³ The broad shoulder of the MLCT excitation band for each of the complexes suggests that they should be amenable to excitation with 405 nm lasers; an excitation wavelength commonly used for confocal laser scanning microscopy.

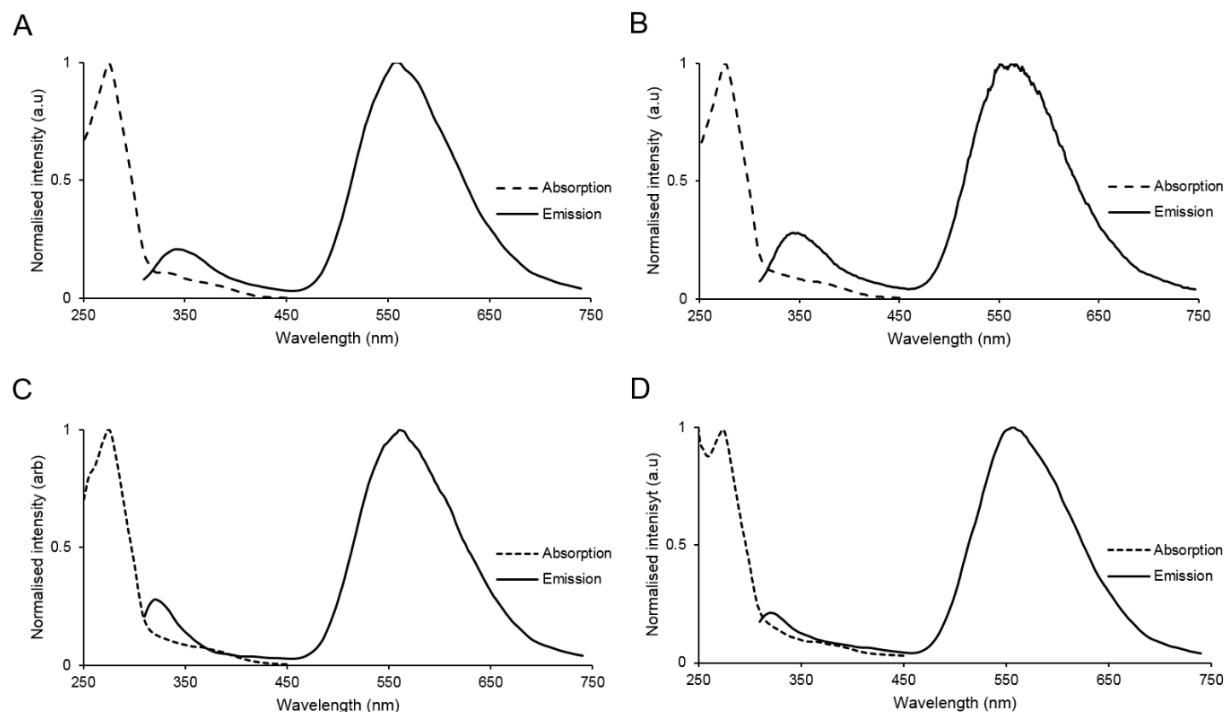


Figure 3. Normalized UV-visible absorption and emission spectra of (A) **ReGlucose** at 5×10^{-6} M; (B) **ReGalactose** at 5×10^{-6} M; (C) **ReMannose** at 5×10^{-5} M; and (D) **ReMaltose** at 5×10^{-5} M in 1:1 MeOH/H₂O. Spectra recorded with a constant ionic strength (I) of 1×10^{-3} M using NaCl, excitation at 275 nm was used for luminescent emission.

To determine whether changes in pH alter the emissive properties of the complexes, their absorption and emission were recorded within a physiologically relevant pH range of 4–8 within in 1:1 MeOH/H₂O (a solution composition initially chosen to ensure complete solubility of the complexes during this analysis). The complexes were evaluated by titration at a constant ionic strength I (NaCl) = 1×10^{-3} M starting at pH 4. The pH was gradually adjusted to pH 8 and then back to pH 4 by micro additions of NaOH and HCl solutions. The complexes were determined to be stable across a biologically relevant pH range and did not display significant changes in MLCT emission under these conditions (ESI Figure S14 and S15 for emission).

Characterization in live cells

The cellular uptake, distribution and cytotoxicity of the carbohydrate-conjugated Re(I) complexes were assessed in H9c2 cardiomyoblasts, which were selected due to their high reliance on carbohydrate metabolism and previous use in toxicity studies.⁴⁴ The total amount of each carbohydrate-conjugated Re(I) complex internalized by H9c2 cells was evaluated quantitatively, using ICP-MS, and is represented in femtograms (fg) per H9c2 cell in **Table 2**. The **ReAlkyne** was included for comparison and demonstrated the highest intercellular concentrations (521 ± 38 fg/cell). Of the carbohydrate-conjugated Re(I) complexes, **ReGlucose** (392 ± 4 fg/cell) had the highest intracellular concentration, followed by **ReMannose** (158 ± 14 fg/cell), **ReMaltose** (72 ± 2 fg/cell) and **ReGalactose**, which had the lowest uptake (30 ± 7 fg/cell). Lipophilicity is known to play an important role in the transport of materials across the cellular membrane by passive diffusion, therefore the $\log D$ value for each complex was determined using the “shake-flask” method,³⁹ at a physiologically-relevant pH (pH 7.4). Lipophilicity was reported as the mean $\log D$ value of three separate determinations, alongside their respective standard deviations **Table 2**.

Table 2. Total Re content of H9c2 cardiomyoblasts stained with Re(I) complexes, compared with the lipophilicity of each complex.

Re(I) complex	Cellular Re fg/cell	Lipophilicity ($\log D_{7.4}$)
Unstained control	0 ± 0	-
ReAlkyne	521 ± 38	1.73 ± 0.05
ReGlucose	392 ± 4	0.94 ± 0.02
ReGalactose	30 ± 7	0.71 ± 0.01
ReMannose	158 ± 14	0.79 ± 0.02

ReMaltose	72 ± 2	-0.17 ± 0.04
------------------	------------	------------------

The incorporation of carbohydrate motifs significantly reduced the lipophilicity of the carbohydrate-conjugated Re(I) complexes when compared to the **ReAlkyne** platform (1.73 ± 0.05). Of the carbohydrate-conjugated complexes, **ReGlucose** exhibited slightly higher $\log D_{7.4}$ (0.94 ± 0.02) than that of **ReGalactose** (0.79 ± 0.02) and **ReMannose** (0.71 ± 0.01). **ReMaltose** exhibited a particularly low $\log D_{7.4}$ (-0.17 ± 0.04), which may be due to the elevated hydrogen-bonding capacity of the disaccharide motif. The decreased internalization of carbohydrate-conjugated Re(I) complexes compared with **ReAlkyne** may correlate with the decreased lipophilicity, as compound internalization generally positively correlates with lipophilicity.^{13, 19, 45} For the monosaccharide carbohydrate-conjugates, this trend was also observed with the most lipophilic members of the series; **ReGlucose** having the highest intercellular accumulation, followed by **ReMannose** and **ReGalactose**. Despite having the lowest lipophilicity, **ReMaltose** had greater intercellular accumulation than **ReGalactose**. This suggests that the $\log D$ value should not be considered as a sole determinant of the cellular membrane permeability, but rather as a contributing factor to total membrane transport. Interestingly, **ReMannose** and **ReGalactose** despite having similar lipophilicity values ($\log D_{7.4}$ 0.79 ± 0.02 and $\log D_{7.4}$ 0.71 ± 0.01 respectively), exhibit a significant difference in total cellular uptake; cells stained with **ReMannose** had a five fold increase complex internalization compared to those stained with **ReGalactose** (158 ± 14 compared to 30 ± 7 fg of Re(I)/cell). This highlights that the substitution of the carbohydrate motif (when the variable of lipophilicity and molecular mass are consistent) may enable cellular internalization of the complex *via* a carbohydrate specific handling mechanism. In light of this hypothesis it is rationalized that the high cellular uptake of **ReGlucose** (521 ± 38 fg of Re(I)/cell)

whilst only slightly higher in lipophilicity ($\log D_{7.4} 0.94 \pm 0.02$) than **ReMannose** and **ReGalactose** could be attributed to the high demand for glucose for cellular metabolism, indicating that the carbohydrate vector is likely contributing to total cellular uptake, not merely passive diffusion relating to the lipophilicity of the complexes.

Carbohydrate-conjugated Re(I) complexes were visualized in H9c2 cells using confocal laser scanning microscopy, with excitation at 403 nm and emission detected from each complex between 545–595 nm. All four complexes were detected in cells following a 30 min incubation period, at concentrations of 2.0×10^{-5} M, 1.0×10^{-4} M and 1.5×10^{-4} M (**Figures 4, S16 and S17**). Detection of carbohydrate-conjugated Re(I) complexes was both time and concentration dependent (**Figure S17**), suggesting uptake may partially be a result of passive diffusion. Similar vesicular distribution was observed for all complexes at 30 minutes and 24 hours, suggesting that the complexes accumulated and were not trafficked out of the cell or degraded by the cell. When compared to the staining pattern of the **ReAlkyne** platform, the attachment of the carbohydrate targeting motif decreased the cytoplasmic localization of the complexes and led to the increase in vesicular accumulation (**Figure 4**). These observations suggest that the addition of the carbohydrate altered the targeting of the complexes. Time-course imaging has shown that the complexes were photostable within cells, resisting photobleaching over a 25 minute illumination (**Figure S18**).

As carbohydrate uptake is primarily mediated through glucose transporters (GLUTs), the transport of carbohydrate-conjugated Re(I) complexes was assessed in the presence of D-glucose (a competitive inhibitor of GLUT-mediated transport). The addition of D-glucose to the cells did not alter the uptake of any of the carbohydrate-conjugated Re(I) complexes (**Figure 4**), suggesting that their internalization was not mediated by GLUTs. In addition, the inhibition or activation of

GLUT1, which is claimed to regulate cellular uptake of mannose,^{23, 46} did not alter the observed uptake of **ReMannose** by H9c2 cells (**Figure S19**). These results contrast those of evaluated carbohydrate appended cationic Re(I) complexes which have been shown to exhibit diminished cellular internalization through competitive inhibition of GLUT transport in the presence of their respective free sugars.^{23, 47} For instance, the inclusion of D-fructose in cell culture media was shown to significantly diminish the cellular uptake of a fructose appended cationic Re(I) complex by specific breast cancer cell lines (MCF-7 and MDA-MB-231) yet not in other cell lines (A549, HepG2, NIH/3T3 and HEK293T) ascribed to a difference in their reliance on GLUT transport.⁴⁷ Similarly, D-glucose was shown to inhibit the uptake of a glucose appended cationic Re(I) complexes by 40% in HeLa cells.²³ Yet, it appears that the internalization of the neutral carbohydrate-conjugated Re(I) complexes is not specifically directed by the carbohydrate targeting motif in H9c2 cells.

To define the intracellular localization of the carbohydrate-conjugated Re(I) complexes, co-staining was performed using organelle labelling dyes to late endosomes/lysosomes (LysoTracker™ Red DND-99) and endoplasmic reticulum (ER; ER-Tracker™ Red) (**Figure 4**; see **Table S3** for co-localization coefficients). Co-localization was detected between all complexes and late endosomes/lysosomes, with the greatest accumulation seen for **ReMannose** and **ReMaltose**. These observations suggest that the changes in carbohydrate targeting motif have altered the intracellular localization of the complexes and may indicate involvement with important biological processes within the cardiomyocyte cells. These results are consistent with the neutral carbohydrate appended dinuclear Re(I) complexes reported by Palmioli *et al.* which have exhibited prominent co-localisation with ER-Tracker™ confirming endosomal localisation.²¹

It is probable that these dinuclear complexes may, similarly to those presented in this study, accumulate to an extent within the lysosome, however this has not explicitly determined.

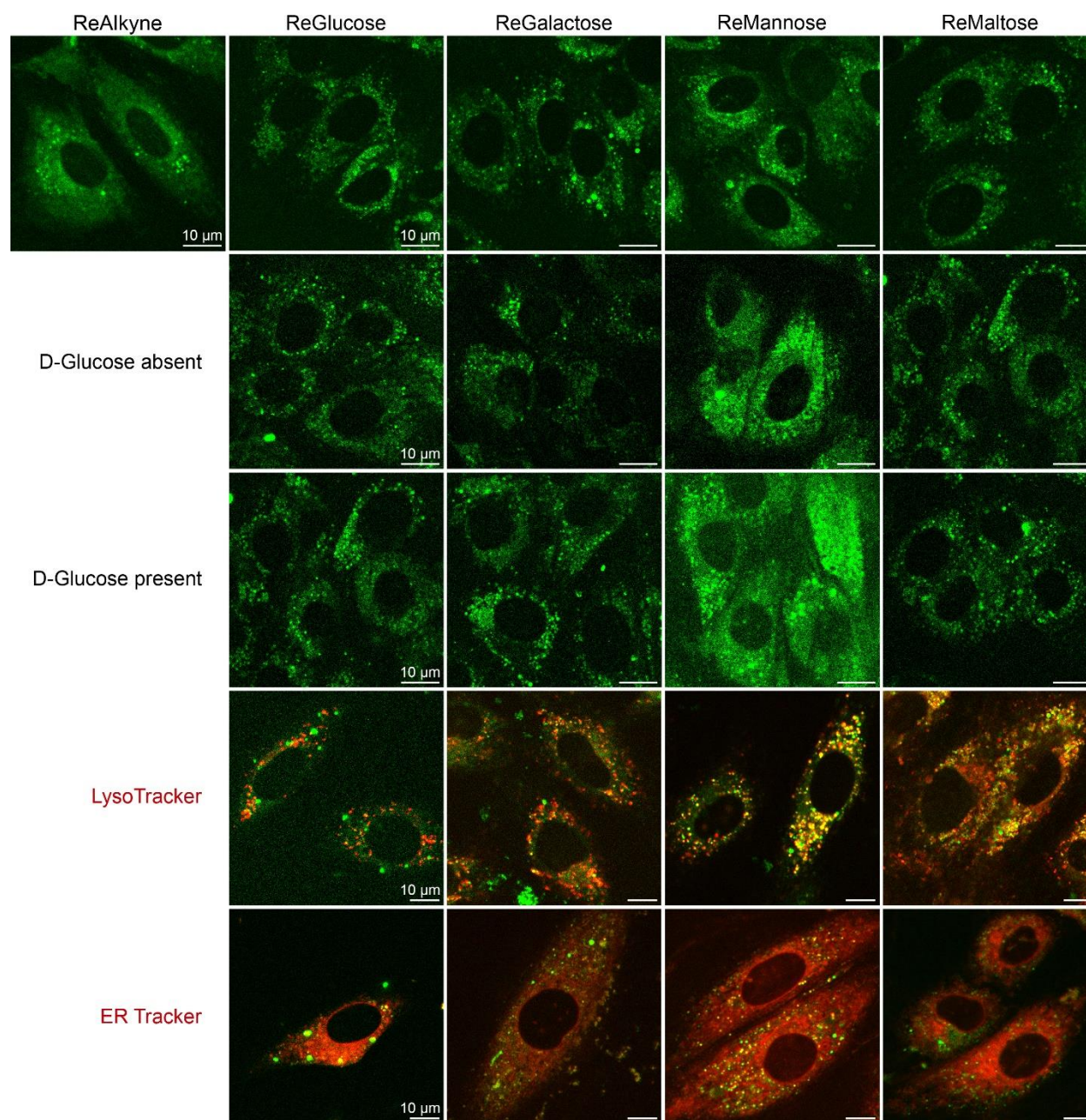


Figure 4. Accumulation of carbohydrate-conjugated Re(I) complexes in H9c2 cells (panel 1). H9c2 cells incubated with carbohydrate-appended Re(I) complexes for 1 hour in the absence (panel 2) or presence (panel 3) of D-glucose. Co-staining of the carbohydrate-appended Re(I)

complexes (green) with LysoTracker™ (red; panel 4) and ER-Tracker™ (red; panel 5), with regions of co-localisation appearing as yellow/orange. Scale bars: 10 µm.

To determine the toxicity profile of the neutral carbohydrate-appended Re(I) complexes, cell viability was assessed by resazurin assay. The carbohydrate complexes exhibited low-level toxicity; a 20-40% decrease in cellular viability was observed following a 24-hour incubation at 1×10^{-4} M (**Figure S20**). However, there were no obvious morphological signs of cytotoxicity in H9c2 cells (**Figure 4**), which would indicate that with some caution these complexes can be used for live cell imaging.

Conclusion

A new neutral “click” conjugatable Re(I) complex platform, **ReAlkyne**, was developed as a biocompatible alternative to previously reported cationic metal complexes. This platform was evaluated by “click” conjugation with benzyl azide to produce a model complex (**ReBn**). Both the **ReAlkyne** platform and **ReBn** were obtained as single crystals which allowed for complete structural elucidation using x-ray crystallography. Four carbohydrate-conjugated neutral Re(I) complexes were then prepared and evaluated as live cell imaging agents, using confocal laser scanning microscopy. The complexes had limited toxicity and were found to enter live cells, with biodistribution to either the late endosomes/lysosomes and/or ER. This contributes a further example of the difference between cationic and neutral carbohydrate complexes; with the former tending toward mitochondrial accumulation,^{10, 13-14} and the latter exhibiting a distribution that is predominantly endosomal.²¹

The four carbohydrate complexes were detected in H9c2 cells, with varying degrees of cellular uptake as quantified by ICP-MS. The lipophilic nature of many ligand systems often enhances the passive membrane diffusion of complexes, but this can at times be a trade-off with respect to

bioavailability and aqueous solubility. Bioconjugated complexes can adopt the targeting potential associated with an attached biomolecule and, being neutral, eliminate a dominant effect of charged groups in the targeting/distribution process. In this study, the cellular localization of the complexes shows that neutral complexes have utility as biocompatible platforms for the development of non-disruptive live cell imaging agents. The sugar motifs did not appear to direct the targeting of the Re(I) complexes to sugar transporters, but rather influenced the biodistribution following passive uptake.

AUTHOR INFORMATION

Corresponding Authors

*E-mail: Sally.Plush@unisa.edu.au

*E-mail: Stefano.Stagni@unibo.it

Author Contributions

The manuscript was written through contributions of all authors.

All authors have given approval to the final version of the manuscript.

Todd A. Gillam – Design of work, data collection, data analysis and interpretation drafting the article, final approval of version to be published.

Chiara Caporale – Design, data collection and data analysis of the preliminary complexes, manuscript editing.

Robert D. Brooks – Design of work, data collection, data analysis, manuscript editing.

Christie A. Bader – Cellular imaging experimental design, data collection and data analysis, manuscript preparation and editing.

Alexandra Sorvina – Data collection, analysis and interpretation, manuscript preparation and editing.

Melissa V. Werrett – Data collection and analysis of the preliminary complex, manuscript editing.

Phillip J. Wright – Data collection and analysis of the preliminary complex, manuscript editing.

Janna L. Morrison – Conception of the study, data interpretation, editing the manuscript.

Massimiliano Massi – Involved in initial concept development (patent), project supervision, experimental design, data interpretation, manuscript writing and editing. Provided intellectual input and project funding for personnel.

Doug A. Brooks – Involved in initial concept development (patent), project supervision, experimental design, data interpretation, manuscript writing and editing. Provided intellectual input and project funding for personnel.

Stefano Zacchini - Single crystal X-ray crystallography: data collection, data analysis and writing of the X-ray crystallography Section.

Shane M. Hickey – Synthesis and characterisation of compounds, data collection and analysis, manuscript editing

Stefano Stagni – Designed concept (patent), supervised project, experimental design, data interpretation, manuscript writing and editing. Provided intellectual input.

Sally E. Plush - Designed concept (patent), supervised project, experimental design, data interpretation, manuscript writing and editing. Provided intellectual input and project funding for personnel.

Funding Sources

Funding for this project was provided by TechinSA (formerly BiotechSA) in partnership with ReZolve Scientific. Funding for this project was also provided by Envision Sciences. JLM was funded by an Australian Research Council Future Fellowship (Level 3; FT170100431).

Acknowledgments

The authors acknowledge the instruments, and scientific and technical assistance provided by Dr Sarah Gilbert at Adelaide Microscopy. Adelaide Microscopy, The University of Adelaide, is a facility that is funded by the University, and State and Federal Governments.

ASSOCIATED CONTENT

Accession Codes: CCDC 2043351 and 2043352 contain the supplementary crystallographic data for this paper. These data can be obtained free of charge via www.ccdc.cam.ac.uk/data_request/cif, or by emailing data_request@ccdc.cam.ac.uk, or by contacting Cambridge Crystallographic Data Centre, 12 Union Road, Cambridge CB2 1EZ, UK; fax: +44 1223 336033

Supporting information: The supporting information is available free of charge as a PDF on the ACS publications website at DOI: xxxxxxxxxxxx. The supporting information contains ¹H and ¹³C NMR spectra, HRMS spectra, tables of associated crystallographic information, as well as absorption and emission spectra of each of the carbohydrate-appended complexes (including spectra associated with pH stability studies).

Conflict of Interest Disclosure

SEP, MM, DAB and SS were all shareholders and co-founders of ReZolve Scientific, a company that has since ceased trading and as such have no conflicting interest, nor to any other authors

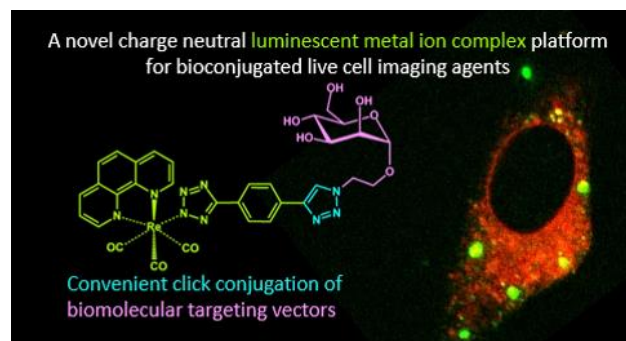
REFERENCES

1. Gottschaldt, M.; Schubert, U. S., Prospects of metal complexes peripherally substituted with sugars in biomedical applications. *Chem. Eur. J.* **2009**, *15* (7), 1548-1557.
2. Lucero, C. G.; Woerpel, K. A., Stereoselective C-glycosylation reactions of pyranoses: the conformational preference and reactions of the mannosyl cation. *J. Org. Chem* **2006**, *71* (7), 2641.
3. Bader, C. A.; Sorvina, A.; Simpson, P. V.; Wright, P. J.; Stagni, S.; Plush, S. E.; Massi, M.; Brooks, D. A., Imaging nuclear, endoplasmic reticulum and plasma membrane events in real time. *FEBS Letters* **2016**, *590* (18), 3051-3060.
4. Coogan, M. P.; Fernández-Moreira, V., Progress with, and prospects for, metal complexes in cell imaging. *ChemComm* **2014**, *50* (4), 384-399.
5. Li, X.; Gorle, A. K.; Ainsworth, T. D.; Heimann, K.; Woodward, C. E.; Grant Collins, J.; Richard Keene, F., RNA and DNA binding of inert oligonuclear ruthenium(ii) complexes in live eukaryotic cells. *Dalton Trans* **2015**, *44* (8), 3594-3603.
6. Li, X.; Heimann, K.; Dinh, X. T.; Keene, F. R.; Collins, J. G., Biological processing of dinuclear ruthenium complexes in eukaryotic cells. *Mol. Biosyst.* **2016**, *12* (10), 3032-3045.
7. Caporale, C.; Bader, C. A.; Sorvina, A.; MaGee, K. D.; Skelton, B. W.; Gillam, T. A.; Wright, P. J.; Raiteri, P.; Stagni, S.; Morrison, J. L., Investigating Intracellular Localisation and Cytotoxicity Trends for Neutral and Cationic Iridium Tetrazolato Complexes in Live Cells. *Chem. Eur. J.* **2017**.
8. Cao, R.; Jia, J.; Ma, X.; Zhou, M.; Fei, H., Membrane localized iridium (III) complex induces endoplasmic reticulum stress and mitochondria-mediated apoptosis in human cancer cells. *J. Med. Chem.* **2013**, *56* (9), 3636-3644.
9. Liu, Y.; Zhang, P.; Fang, X.; Wu, G.; Chen, S.; Zhang, Z.; Chao, H.; Tan, W.; Xu, L., Near-infrared emitting iridium(iii) complexes for mitochondrial imaging in living cells. *Dalton Trans* **2017**, *46* (14), 4777-4785.
10. Lo, K. K.-W., Luminescent rhenium (I) and iridium (III) polypyridine complexes as biological probes, imaging reagents, and photocytotoxic agents. *Acc. Chem. Res.* **2015**, *48* (12), 2985-2995.
11. Yang, J.; Zhao, J.-X.; Cao, Q.; Hao, L.; Zhou, D.; Gan, Z.; Ji, L.-N.; Mao, Z.-W., Simultaneously Inducing and Tracking Cancer Cell Metabolism Repression by Mitochondria-Immobilized Rhenium(I) Complex. *ACS Appl. Mater. Interfaces* **2017**, *9* (16), 13900-13912.
12. Gillam, T. A.; Sweetman, M. J.; Bader, C. A.; Morrison, J. L.; Hayball, J. D.; Brooks, D. A.; Plush, S. E., Bright lights down under: Metal ion complexes turning the spotlight on metabolic processes at the cellular level. *Coord. Chem. Rev.* **2017**, *375*, 234-255.
13. Louie, M. W.; Liu, H. W.; Lam, M. H. C.; Lam, Y. W.; Lo, K. K. W., Luminescent Rhenium (I) Polypyridine Complexes Appended with an α -D-Glucose Moiety as Novel Biomolecular and Cellular Probes. *Chem. Eur. J.* **2011**, *17* (30), 8304-8308.

14. Lo, K. K.-W.; Law, W. H.-T.; Chan, J. C.-Y.; Liu, H.-W.; Zhang, K. Y., Photophysical and cellular uptake properties of novel phosphorescent cyclometalated iridium (III) bipyridine D-fructose complexes. *Metallomics* **2013**, *5* (7), 808-812.
15. Liu, H.-W.; Zhang, K. Y.; Law, W. H.-T.; Lo, K. K.-W., Cyclometalated iridium (III) bipyridine complexes functionalized with an N-methylamino-oxy group as novel phosphorescent labeling reagents for reducing sugars. *Organometallics* **2010**, *29* (16), 3474-3476.
16. Lee, L. C.-C.; Leung, K.-K.; Lo, K. K.-W., Recent development of luminescent rhenium (I) tricarbonyl polypyridine complexes as cellular imaging reagents, anticancer drugs, and antibacterial agents. *Dalton Trans* **2017**, *46* (47), 16357-16380.
17. Thorp-Greenwood, F. L.; Balasingham, R. G.; Coogan, M. P., Organometallic complexes of transition metals in luminescent cell imaging applications. *J. Organomet. Chem.* **2012**, *714* (0), 12-21.
18. Bader, C.; Carter, E.; Safitri, A.; Simpson, P.; Wright, P.; Stagni, S.; Massi, M.; Lay, P.; Brooks, D.; Plush, S., Unprecedented staining of polar lipids by a luminescent rhenium complex revealed by FTIR microspectroscopy in adipocytes. *Mol. Biosyst.* **2016**, *12* (7), 2064-2068.
19. Bader, C. A.; Brooks, R. D.; Ng, Y. S.; Sorvina, A.; Werrett, M. V.; Wright, P. J.; Anwer, A. G.; Brooks, D. A.; Stagni, S.; Muzzioli, S., Modulation of the organelle specificity in Re (I) tetrazolato complexes leads to labeling of lipid droplets. *RSC Advances* **2014**, *4* (31), 16345-16351.
20. Bader, C. A.; Shandala, T.; Carter, E. A.; Ivask, A.; Guinan, T.; Hickey, S. M.; Werrett, M. V.; Wright, P. J.; Simpson, P. V.; Stagni, S., A molecular probe for the detection of polar lipids in live cells. *PloS one* **2016**, *11* (8), e0161557.
21. Palmioli, A.; Aliprandi, A.; Septiadi, D.; Mauro, M.; Bernardi, A.; De Cola, L.; Panigati, M., Glyco-functionalized dinuclear rhenium (I) complexes for cell imaging. *Org. Biomol. Chem.* **2017**, *15* (7), 1686-1699.
22. Palmioli, A.; Panigati, M.; Bernardi, A., Glycodendron-rhenium complexes as luminescent probes for lectin sensing. *Org. Biomol. Chem.* **2018**, *16* (37), 8413-8419.
23. Law, W. H.-T.; Lee, L. C.-C.; Louie, M.-W.; Liu, H.-W.; Ang, T. W.-H.; Lo, K. K.-W., Phosphorescent Cellular Probes and Uptake Indicators Derived from Cyclometalated Iridium(III) Bipyridine Complexes Appended with a Glucose or Galactose Entity. *Inorg. Chem.* **2013**, *52* (22), 13029-13041.
24. Brooks, R.; Du, Z.; Borlace, G.; Brooks, D.; Plush, S., Synthesis and Characterisation of First Generation Luminescent Lanthanide Complexes Suitable for Being Adapted for Uptake via the Mannose Receptor. *J. Inorg. Chem.* **2013**, *2013*.
25. Palmioli, A.; Panigati, M.; Bernardi, A., Glycodendron-rhenium complexes as luminescent probes for lectin sensing. *Organic & biomolecular chemistry* **2018**, *16* (37), 8413-8419.
26. Kuznetsov, A. V.; Javadov, S.; Sickinger, S.; Frotschnig, S.; Grimm, M., H9c2 and HL-1 cells demonstrate distinct features of energy metabolism, mitochondrial function and sensitivity to hypoxia-reoxygenation. *Biochimica et Biophysica Acta (BBA) - Molecular Cell Research* **2015**, *1853* (2), 276-284.
27. Gottlieb, H. E.; Kotlyar, V.; Nudelman, A., NMR Chemical Shifts of Common Laboratory Solvents as Trace Impurities. *The Journal of Organic Chemistry* **1997**, *62* (21), 7512-7515.
28. Koguro, K.; Oga, T.; Tokunaga, N.; Mitsui, S.; Orita, R., Process for preparation of 5-substituted tetrazoles. Google Patents: 1998.

29. Albertino, A.; Garino, C.; Ghiani, S.; Gobetto, R.; Nervi, C.; Salassa, L.; Rosenberg, E.; Sharmin, A.; Viscardi, G.; Buscaino, R., Photophysical properties and computational investigations of tricarbonylrhenium (I)[2-(4-methylpyridin-2-yl) benzo [d]-X-azole] L and tricarbonylrhenium (I)[2-(benzo [d]-X-azol-2-yl)-4-methylquinoline] L derivatives (X= N-CH₃, O, or S; L= Cl⁻, pyridine). *J. Organomet. Chem.* **2007**, 692 (6), 1377-1391.
30. Kalyanasundaram, K., Luminescence and redox reactions of the metal-to-ligand charge-transfer excited state of tricarbonylchloro-(polypyridyl) rhenium (I) complexes. *J. Chem. Soc. Faraday Trans. 2: Molecular and Chemical Physics* **1986**, 82 (12), 2401-2415.
31. Quagliotto, P.; Viscardi, G.; Barolo, C.; D'Angelo, D.; Barni, E.; Compari, C.; Duce, E.; Fisicaro, E., Synthesis and properties of new glucocationic surfactants: model structures for marking cationic surfactants with carbohydrates. *J. Org. Chem.* **2005**, 70 (24), 9857-9866.
32. Coles, H. W.; Bergeim, F. H., Halogeno-alkyl Glycosides. III. Quaternary Salts. Glucosamine Quaternary Derivative. *J. Am. Chem. Soc.* **1938**, 60 (6), 1376-1379.
33. Hayes, W.; Osborn, H. M.; Osborne, S. D.; Rastall, R. A.; Romagnoli, B., One-pot synthesis of multivalent arrays of mannose mono-and disaccharides. *Tetrahedron* **2003**, 59 (40), 7983-7996.
34. Yoon, S.; Ho Hwang, S.; Bae Ko, W., Sonochemical Reaction of Fullerene [C₆₀] with Several 2'-Azidoethyl per-O-Acetyl Glycosides. *Journal of Nanoscience and Nanotechnology* **2008**, 8 (6), 3136-3141.
35. Pathak, A. K.; Pathak, V.; Riordan, J. M.; Gurucha, S. S.; Besra, G. S.; Reynolds, R. C., Synthesis of mannopyranose disaccharides as photoaffinity probes for mannosyltransferases in Mycobacterium tuberculosis. *Carbohydrate Research* **2004**, 339 (3), 683-691.
36. Sheldrick, G. M., SHELXT-Integrated space-group and crystal-structure determination. *Acta Crystallographica Section A: Foundations and Advances* **2015**, 71 (1), 3-8.
37. Demas, J.; Crosby, G. A., Measurement of photoluminescence quantum yields-Review. *Journal of Physical Chemistry* **1971**, 75 (8), 991-&.
38. Suzuki, K.; Kobayashi, A.; Kaneko, S.; Takehira, K.; Yoshihara, T.; Ishida, H.; Shiina, Y.; Oishi, S.; Tobita, S., Reevaluation of absolute luminescence quantum yields of standard solutions using a spectrometer with an integrating sphere and a back-thinned CCD detector. *Phys. Chem. Chem. Phys.* **2009**, 11 (42), 9850-9860.
39. Kunz, P. C.; Huber, W.; Rojas, A.; Schatzschneider, U.; Spingler, B., Tricarbonylmanganese (I) and-rhenium (I) Complexes of Imidazol-Based Phosphane Ligands: Influence of the Substitution Pattern on the CO Release Properties. *Eur. J. Inorg. Chem.* **2009**, 2009 (35), 5358-5366.
40. Mede, T.; Jäger, M.; Schubert, U. S., "Chemistry-on-the-complex": functional Ru II polypyridyl-type sensitizers as divergent building blocks. *Chem. Soc. Rev.* **2018**, 47 (20), 7577-7627.
41. Werrett, M. V.; Chartrand, D.; Gale, J. D.; Hanan, G. S.; MacLellan, J. G.; Massi, M.; Muzzioli, S.; Raiteri, P.; Skelton, B. W.; Silberstein, M., Synthesis, structural, and photophysical investigation of diimine tricarbonyl Re (I) tetrazolato complexes. *Inorg. Chem.* **2011**, 50 (4), 1229-1241.
42. Pulsipher, A.; Yousaf, M. N., A renewable, chemoselective, and quantitative ligand density microarray for the study of biospecific interactions. *Chemical Communications* **2011**, 47 (1), 523-525.
43. Croce, A. C.; Bottioli, G., Autofluorescence Spectroscopy and Imaging: A Tool for Biomedical Research and Diagnosis. *Eur J Histochem.* **2014**, 58 (4), 2461.

44. Pereira, S. L.; Ramalho-Santos, J.; Branco, A. F.; Sardao, V. A.; Oliveira, P. J.; Carvalho, R. A., Metabolic remodeling during H9c2 myoblast differentiation: relevance for in vitro toxicity studies. *Cardiovasc. Toxicol.* **2011**, *11* (2), 180-190.
45. Puckett, C. A.; Ernst, R. J.; Barton, J. K., Exploring the cellular accumulation of metal complexes. *Dalton Trans* **2010**, *39* (5), 1159-1170.
46. Panneerselvam, K.; Freeze, H. H., Mannose enters mammalian cells using a specific transporter that is insensitive to glucose. *J. Biol. Chem* **1996**, *271* (16), 9417-9421.
47. Yin Zhang, K.; Ka-Shun Tso, K.; Louie, M.-W.; Liu, H.-W.; Kam-Wing Lo, K., A Phosphorescent Rhenium(I) Tricarbonyl Polypyridine Complex Appended with a Fructose Pendant That Exhibits Photocytotoxicity and Enhanced Uptake by Breast Cancer Cells. *Organometallics* **2013**, *32* (18), 5098-5102.



For Table of Contents Only

Snyopsis for TOC: Exploring the effect of conjugating four different carbohydrate moieties to a neutral Re(I) alkyne platform has on lipophilcity, cellular uptake and localisation in the quest for new live cell imaging agents.